

A Synoptic- and Remote Sensing-based Analysis of a Severe Dust Storm Event over Central Asia

Parya Broomandi^{1,12†}, Kaveh Mohammadpour^{2,3†}, Dimitris G. Kaskaoutis⁴,
Aram Fathian^{5,6,7}, Sabur F. Abdullaev⁸, Vladimir A. Maslov⁸,
Amirhossein Nikfal⁹, Ali Jahanbakhshi¹⁰, Bakhyt Aubakirova¹,
Jong Ryeol Kim^{1*}, Alfrendo Satyanaga¹, Alireza Rashki¹¹, Nick Middleton¹³

¹Department of Civil and Environmental Engineering, School of Engineering and Digital Sciences, Nazarbayev University, Astana 010000, Kazakhstan

²Department of Climatology, Faculty of Geographical Sciences, Kharazmi University, Tehran, Iran

³Climate Change Technology Transfer to Developing Countries Group (SSPT-PVS), Department of Sustainability, Italian National Agency for New Technologies Energy and Sustainable Development, ENEA, C. R. Casaccia, 00123 Rome, Italy

⁴Institute for Environmental Research and Sustainable Development, National Observatory of Athens, 15236 Athens, Greece

⁵UNESCO Chair on Coastal Geo-Hazard Analysis, Research Institute for Earth Sciences, Tehran, Iran

⁶Neotectonics and Natural Hazards Institute, RWTH Aachen University, Aachen, Germany

⁷Water, Sediment, Hazards, and Earth-surface Dynamics (waterSHED) Lab, Department of Geoscience, University of Calgary, Canada

⁸Department of Physical Atmosphere, Physical-Technical Institute, Academy of Sciences of Republic of Tajikistan, 734063, Dushanbe, Tajikistan

⁹Atmospheric Science and Meteorological Research Centre (ASMRC), Tehran, Iran

¹⁰School of Architecture, Building and Civil Engineering, Loughborough University, Loughborough, UK

¹¹Department of Desert and Arid Zones Management, Ferdowsi University of Mashhad, Mashhad, Iran

¹²Department of Chemical Engineering, Masjed-Soleiman Branch, Islamic Azad University, Masjed-Soleiman, Iran

¹³St Anne's College, University of Oxford, Oxford OX2 6HS, UK

OPEN ACCESS



Received: September 1, 2022

Revised: December 6, 2022

Accepted: January 3, 2023

* Corresponding Author:

jong.kim@nu.edu.kz

† These authors contributed equally to this work

Publisher:

Taiwan Association for Aerosol Research

ISSN: 1680-8584 print

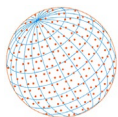
ISSN: 2071-1409 online

© Copyright: The Author(s).

This is an open access article distributed under the terms of the [Creative Commons Attribution License \(CC BY 4.0\)](https://creativecommons.org/licenses/by/4.0/), which permits unrestricted use, distribution, and reproduction in any medium, provided the original author and source are cited.

ABSTRACT

A severe dust storm blanketing Central Asia on 3–4 November 2021 was investigated employing satellite remote-sensing, synoptic meteorological observations, reanalysis and HYSPLIT back-trajectories. The prevailing meteorological conditions showed an intensification of air subsidence over eastern Kazakhstan, featured in a typical omega-blocking system over the region and two troughs to its west and east axis, one day before the dust storm. The prevailing high-pressure system and temperature gradients over Kazakhstan modulated the dominant anticyclonic wind pattern generated from the south Balkhash basin toward the Caspian Sea, causing a huge dust storm that covered the southern half of Kazakhstan and large parts of Uzbekistan, Tajikistan and Turkmenistan. The dust storm originated in the steppes of southern Kazakhstan by violent downdraft winds. Initially it swept over eastern parts and then the whole of Uzbekistan, reaching the Caspian Sea in the west. Meteorological measurements and HYSPLIT back-trajectories at selected sites in Central Asia (Turkmenabat, Khujand and Tashkent) showed a remarkable dust impact that reduced temperature (by 2–4°C) and visibility to below 1 km at different periods, as the thick dust plume expanded in various directions. The extremely high PM concentrations ($PM_{10} > 10,000 \mu g m^{-3}$ in Tashkent) could endanger both human health and the environment, especially in a region suffering from high susceptibility to wind erosion and significant land



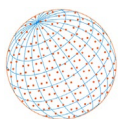
degradation and desertification. Effective and immediate stabilising measures to control wind erosion in vulnerable areas of Central Asia are warranted.

Keywords: Atmospheric circulation, Dust storms, HYSPLIT, Backward trajectory, Tashkent

1 INTRODUCTION

The ambient air pollution induced by dust storms is associated with a wide range of human health disorders (Middleton, 2020) including (i) respiratory diseases such as bronchial asthma and chronic bronchitis (Al-Hemoud *et al.*, 2018; Kang *et al.*, 2012; Wang *et al.*, 2014), (ii) cardiovascular diseases (Aghababaeian *et al.*, 2021; Aili and Kim Oanh, 2015), (iii) psychological and cognitive disorders (Ghaisas *et al.*, 2016; Gordeev *et al.*, 2013) and (iv) neurodegenerative diseases (Aleya and Uddin, 2020; Chin-Chan *et al.*, 2015; Galán-Madruga *et al.*, 2020; Galán-Madruga and García-Camero, 2022; Shafiee *et al.*, 2021). Moreover, increased total non-accidental deaths in both adults and children are reported among exposed individuals in areas highly impacted by dust storms (Achilleos *et al.*, 2019; Díaz *et al.*, 2017; Galán-Madruga *et al.*, 2022; Kashima *et al.*, 2016; Perez *et al.*, 2008). High ambient concentrations of dust particles caused by intense dust storms also lead to horizontal visibility reduction, which can have socio-economic impacts in several sectors, including aviation, transport, education, leisure construction and energy production (Middleton *et al.*, 2021; Middleton, 2017; Middleton and Kang, 2017). Dust aerosols, originating from desert areas all over the world, can play an important role in altering Earth's solar radiation balance and the primary productivity of oceans through iron fertilization (Jickells *et al.*, 2005; Kok *et al.*, 2018; Schepanski, 2018). Dust is a major type of tropospheric aerosol and the most common wind-induced climatic phenomenon in the hyperarid, arid and semi-arid regions of Central Asia (CA), accounting for ~25% of total global dust emissions, with significant impacts on regional climate, biogeochemical cycles, loess formation and the hydrological cycle (Booth *et al.*, 2012; Ginoux *et al.*, 2004; Li *et al.*, 2021; Issanova and Abuduwaili, 2017; Uno *et al.*, 2009).

In recent times, dust generation and, consequently, population exposure in CA have escalated due to climate variability and land cover changes, as a result of rapid development, deforestation, enhanced aridity, mining and agricultural activities (Gao and Washington, 2009; Sternberg and Edwards, 2017; UN, 2010; Wiggs *et al.*, 2003). Across CA, the most wind erosive areas and hotspots of dust storm activity are in Kazakhstan (areas surrounding the desiccated Aral Sea, known as the Aralkum Desert, Saryesik Atyrau Desert to the south of Lake Balkhash and Muyunkum Desert to its western end), Turkmenistan (Karakum Desert), Uzbekistan (Kyzylkum Desert), west of Mongolia and northwest China (Tarim Basin, Taklimakan and Gurbantunggut Deserts) (Gholami *et al.*, 2021; Laurent *et al.*, 2006; Song *et al.*, 2021). Beyond climate change (decrease of precipitation and desertification over CA), human intervention, specifically the extended cultivation ploughing up of pastures during the Virgin Lands Programme of the 1950s, have played an important role in the increased wind erosion activity (Goudie and Middleton, 2006; Indoitu *et al.*, 2012). For example, in Kazakhstan, different degrees of land degradation and desertification occur due to anthropogenic activities, unsustainable land practices such as agricultural activities, and non-rational use of natural sources such as water (Almaganbetov and Grigoruk, 2008; MARK, 2006; Lau *et al.*, 2020; Madruga *et al.*, 2019). Land degradation and desertification are mainly observed in regions under unfavourable ecological conditions such as Lake Balkhash, Caspian lowland and around the dried bed of the Aral Sea (GEF, 2003; NPRK, 2005). The areas in Kazakhstan most vulnerable to wind erosion are the western and southern parts, where the total wind-eroded lands are estimated at about 12.4 and 13.1 million hectares respectively (out of 273.5 million hectares of the Kazakhstan territory). In addition, wind eroded agricultural lands in the eastern and northern parts of the country occupy about 1.28 and 3.87 million hectares respectively, which are subject to accelerated desertification, including around 66% of Kazakhstan's total area (Almaganbetov and Grigoruk, 2008; CSD, 2002). These conditions may lead to changes in regional terrestrial (desertification, wetness of topsoil, surface water resources, surface roughness) and climatic factors (wind and rainfall regimes), facilitating generation of dust storms over CA (Huang *et al.*, 2016, 2017; Mahmoodirad and Sanei, 2016; Wang *et al.*, 2017; Xi and Sokolik, 2015).



Seasonal and inter-annual changes in atmospheric circulation patterns, along with changes in local topography, land use land cover (LULC) and long-term modulations of the climate system, control the dust activity over CA (Kaskaoutis *et al.*, 2017; Nobakht *et al.*, 2021; Shi *et al.*, 2019; Zhang *et al.*, 2020). Dust particles rising from Central Asia are held responsible for air-quality deterioration over Korea, Japan and Taiwan (Hashizume *et al.*, 2010; Hasunuma *et al.*, 2019), as well as northeast Iran-Afghanistan and other parts of southwest Asia (Kaskaoutis *et al.*, 2016; Mohammadpour *et al.*, 2022). Specific synoptic weather patterns may also favour dust from CA to be transported to the west, impacting Georgia, Belarus and Lithuania (Hongisto and Sofiev, 2004) or even the Balkans and Italy (Tositti *et al.*, 2022). Furthermore, other studies showed that 3% of Asian dust can reach the western USA (Creamean *et al.*, 2014). Dust-raising activity over CA occurs mostly during spring and summer, depending on area and meteorological conditions (Rupakheti *et al.*, 2020, 2019), while dust-induced radiative forcing during intense dust events in Dushanbe, Tajikistan were estimated at -48 ± 12 , -85 ± 24 and $37 \pm 15 \text{ Wm}^{-2}$ at the top of the atmosphere, surface and within the atmosphere, respectively, with even higher values during extreme dust events (Rupakheti *et al.*, 2021). Although several aspects regarding dust sources, climatology of dust activity and dust impacts have been well documented in CA, as discussed above, case studies of severe and long-range transported dust events from this region are rare in the literature (Tositti *et al.*, 2022).

This work analyses a severe dust storm event over CA that affected a large area in southern Kazakhstan, Uzbekistan and Tajikistan on 3–4 November 2021 (Eurasianet, 2021; MKWEATHER, 2021) (Fig. 1). A massive dust storm covered Tashkent, the capital of Uzbekistan, where the horizontal visibility decreased to 200 meters and the PM_{10} concentrations spiked at $18,000 \mu\text{g m}^{-3}$ on 4 November 2021, 30 times above the Uzbekistan maximum acceptable level. Local authorities reported that it was the most extreme sand/dust storm during the last 150 years of monitoring in Tashkent (Uzhydromet, 2021). The true colour imagery of Terra-MODIS sensor, accessible from NASA Worldview (<https://worldview.earthdata.nasa.gov>) on 4 November 2021, showed a thick dust plume covering parts of south-eastern Kazakhstan, Uzbekistan and north Tajikistan around the Fergana valley (Fig. 1). People in Tashkent were advised to stay indoors, avoiding walks and

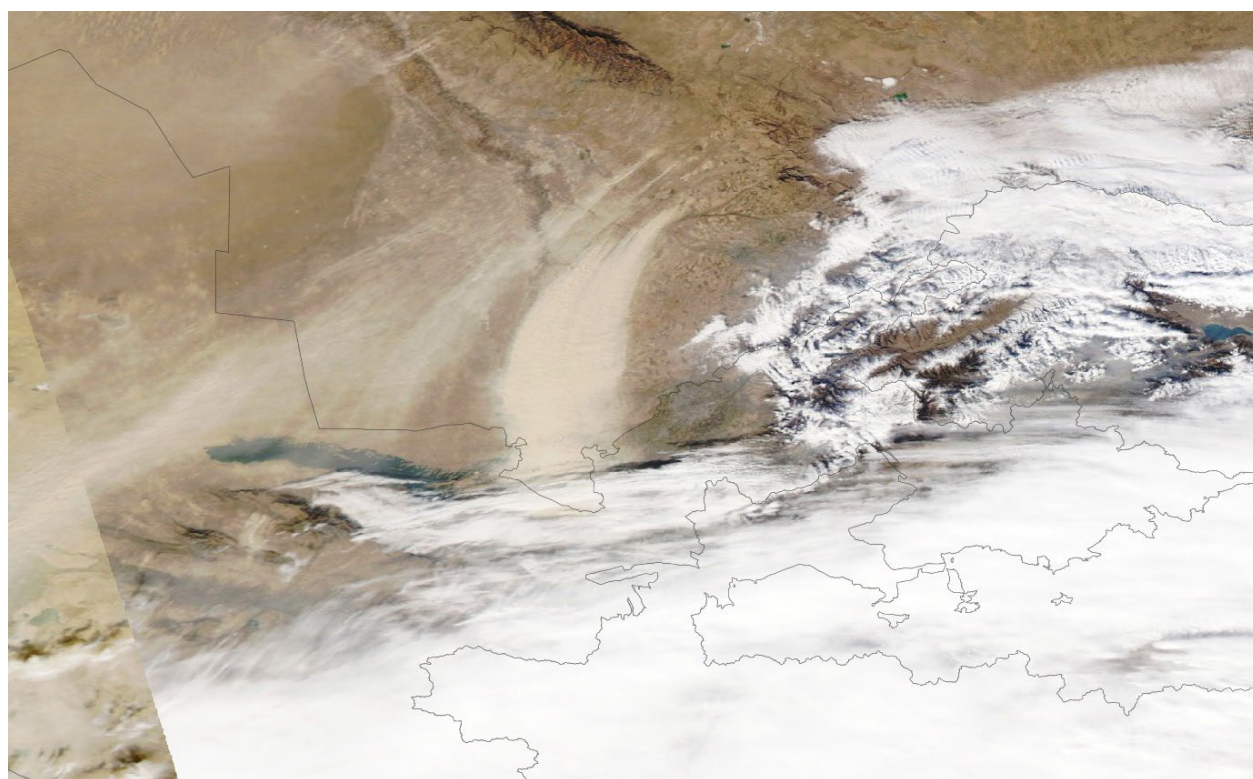
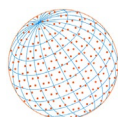


Fig. 1. True colour image from the Terra-MODIS sensor (<https://worldview.earthdata.nasa.gov>) on 4 November 2021, focused on the dust storm.



physical activities. On 4 November 2021, the ambulance service received 687 calls from inhabitants in Tashkent seeking help for respiratory problems. Besides hospital admissions, local authorities reported car accidents and casualties due to low horizontal visibility (Uzhydromet, 2021). Moreover, on 5 November, the dust haze caused interruptions in drinking water supply in some districts of Tashkent due to the malfunction in the high-voltage power supply network (Eurasianet, 2021). Dust intrusion also caused a power outage in about 50 villages in the Turkestan region, southeast Kazakhstan, while drivers were stuck on the highway in traffic jams on 4 November 2021, due to reduced visibility (Eurasianet, 2021). Overall, this severe dust storm caused many socio-economic and health impacts for local inhabitants, beyond deterioration of air quality.

This unprecedented dust event in CA undoubtedly needs further investigation of the meteorological conditions and driving mechanisms that initiated such a dust storm. This study investigates the synoptic meteorology and atmospheric circulation patterns that triggered this dust storm event and aims to detect the dust source and the expansion of the dust plumes via SEVIRI satellite imagery. Furthermore, it examines the impact of the dust storm on local meteorological conditions and visibility at specific sites in CA, and provides discussions about land degradation and increased dust activity over CA during the last decades.

2 METHODS

2.1 Study Region

The Central Asian plains stretch from the shores of the Caspian Sea in the west to the foothills of Altai, Tian-Shan and Pamir Mountains in the east (Fig. 2). The Central Asian drylands cover an area of 1.890 million km² and are home to about 40 million inhabitants (Indoitu *et al.*, 2012). The area consists of various litho-edaphic desert types such as gravel-gypseous and gravel, sandy, sandy-pebble and pebble, loess, loamy, solonchakous and clayey deserts (Issanova and Abuduwaili, 2017; Gholami *et al.*, 2021; Li *et al.*, 2021). Based on different synoptic processes and meteorological conditions, CA is divided into two climatic zones of northern and southern (Issanova *et al.*, 2015). The northern part has a dry and cold continental Central Asian climate, while the southern region is characterized by a dry and hot climate. In the northern part, the mean annual temperature varies between 5 and 11°C, while it increases to 13–16.6°C in the southern part. The annual precipitation over the whole region varies between 80 mm and 200 mm and it is below 100 mm in the desert regions of western Balkash shore, Kyzylkum, Karakum Deserts and Betpak-Dala (Indoitu *et al.*, 2012; Issanova and Abuduwaili, 2017).

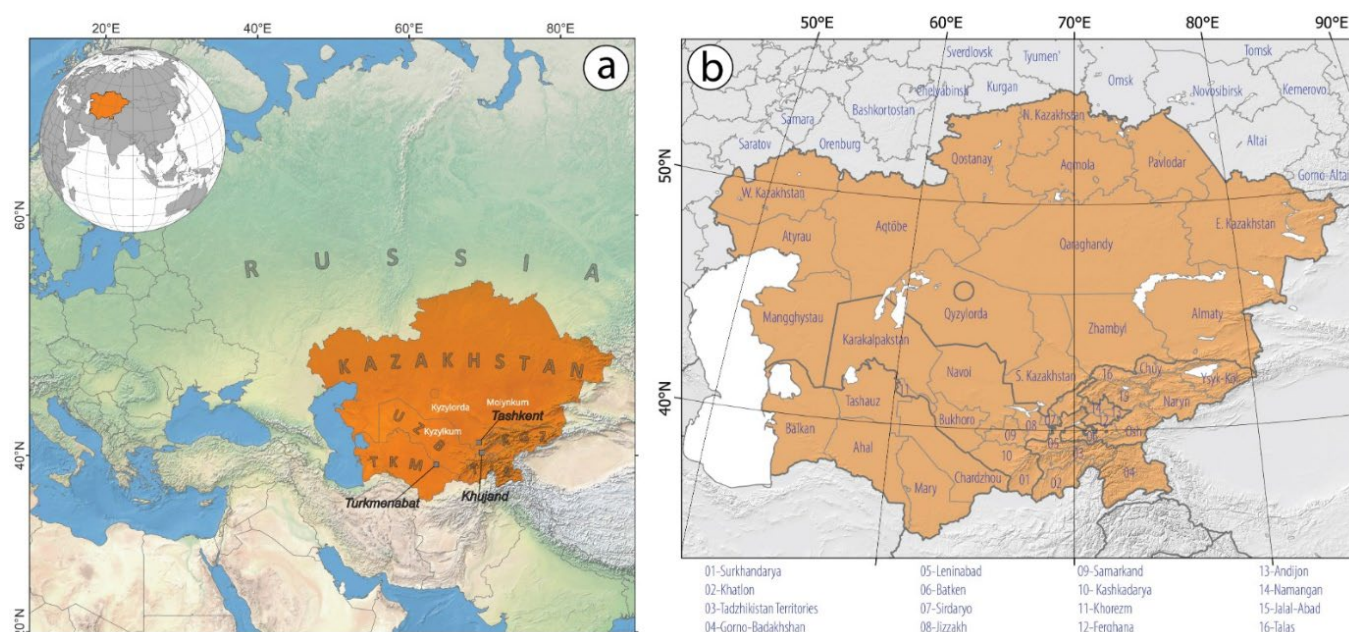
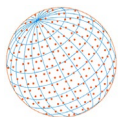


Fig. 2. Physiographic map of the study area highlighting the Central Asian countries.



2.2 Ground-based Observations

In this study, ground-based hourly data of horizontal visibility, wind speed and temperature at selected stations in Central Asia (i.e., Tashkent, Uzbekistan; Khujand, Tajikistan; Turkmenabat, Turkmenistan) were obtained from the Iowa Environmental Mesonet (<https://mesonet.agron.iastate.edu/ASOS/>). Additionally, hourly PM_{2.5} data were obtained from the monitoring station in the United States Embassy in Tashkent, Uzbekistan (<https://www.airnow.gov/international/us-embassies-and-consulates/>).

2.3 Reanalysis Data

ERA-5 reanalysis (Hersbach *et al.*, 2020) is produced by European Centre for Medium-Range Weather Forecasts (ECMWF) within the Copernicus Climate Change Service (C3S), which includes a detailed record of the global atmosphere and land surface from 1950 onwards (Hersbach *et al.*, 2020). In this study, ERA-5 reanalysis data was used to obtain meteorological variables of (i) vertical velocity at 300 hPa, (ii) zonal wind at 250 hPa, (iii) geopotential heights at 500 and 850 hPa, (iv) air temperature at 2 m, (v) Mean Sea Level Pressure (MSLP) and (vi) surface vector winds, for the characterization of the daily synoptic conditions at $0.5^\circ \times 0.5^\circ$ spatial resolution over CA during the dust storm event.

The Modern-Era Retrospective Analysis for Research and Applications, version 2 (MERRA-2), is a long-term global reanalysis product with a horizontal resolution of $0.5^\circ \times 0.625^\circ$ (latitude, longitude) and a temporal resolution varying from hour to month (Galán-Madruga, 2022; Gelaro *et al.*, 2017; Sayer *et al.*, 2019; Shafiee *et al.*, 2019). In this study, the dust loading/dust column mass density (g m^{-2}) was taken over CA on a daily basis around the dust storm event, as MERRA-2 has been proved as an accurate database for studying dust aerosols (Shaheen *et al.*, 2020; Shi *et al.*, 2019; Mahmoodirad *et al.*, 2019).

2.4 Satellite Remote Sensing Observations/Products

Visible/IR images of SEVIRI (Spinning Enhanced Visible and Infrared Imager) were employed to monitor the transport of the dust storm in high temporal resolution (~ 15 mins) (Schepanski *et al.*, 2007, 2009). The infrared channel data from SEVIRI is based on RGB (red-green-blue) image compositions, and dusty pixels in pink or magenta colours are used to monitor the evolution of dust events during both day and night over desert areas (Martínez *et al.*, 2009; Kaskaoutis *et al.*, 2019).

2.5 HYSPLIT Model

The HYSPLIT-4 (Hybrid Single-Particle Lagrangian Integrated Trajectory) model is widely used for analysis of the air-mass trajectories, dispersion and deposition of aerosols using the Global Forecast System (GFS) meteorological parameters as the initial background field (Ashrafi *et al.*, 2014; Draxler and Hess, 1997). In this study, HYSPLIT air-mass back-trajectories were used at certain receptor sites in Central Asia like Tashkent (41.3°N , 69.26°E), Khujand (40.28°N , 69.63°E) and Turkmenabat (39.03°N , 63.56°E) on the dust storm day (4 November 2021), in order to investigate the dust source and the pathways of the expanded dust plumes that affected several regions in Central Asia (Rashki *et al.*, 2015).

3 RESULTS AND DISCUSSION

3.1 Satellite Remote Sensing Observations

SEVIRI Visible/IR imagery enables detection of slight or thick dust plumes, as well as subtle variations from one image to another, on high temporal resolution (Schepanski *et al.*, 2009; Molla-Alizadeh-Zavardehi *et al.*, 2014). In this study, SEVIRI imagery was deployed to monitor the evolution of the dust storm, aiming to identify the source origin, expansion of the dust plume and the affected areas in CA on 4 November 2021 (Fig. 3). Strong north-easterlies, which will be analysed in the next section, triggered dust-raising in Zhambyl region, and activated dust sources in Moiyunkum, Kyzylorda and eastern Kyzylkum Deserts in the early morning of 4 November 2021 (04:00 UTC). The thick dust plume, shown in bold pink and magenta colours, reached Turkmenabat, Tashkent

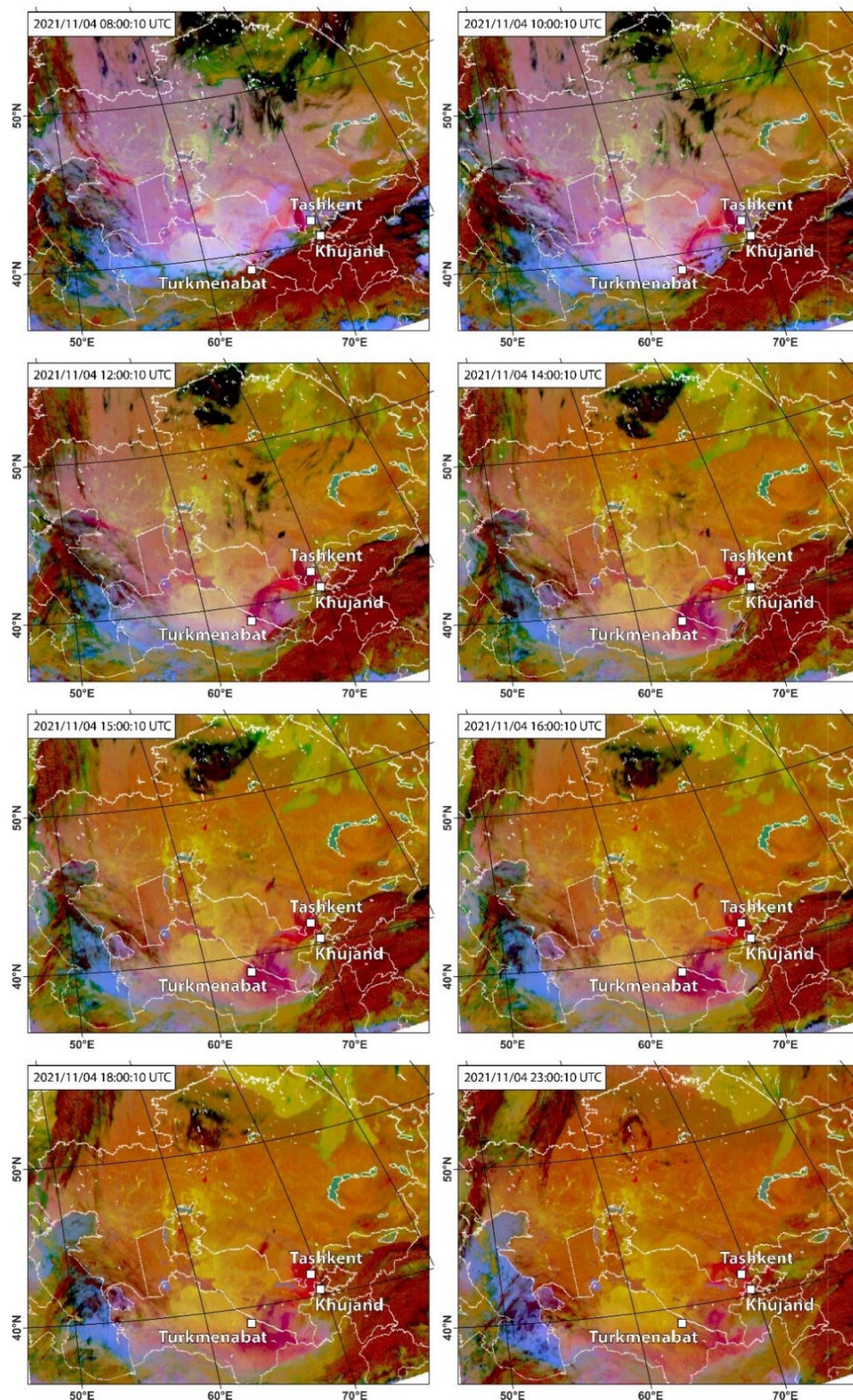
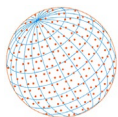
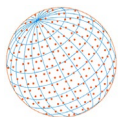


Fig. 3. SEVIRI satellite images over Central Asia at different hours on 4 November 2021, detecting the evolution of the thick dust plume (in pink/magenta). The key receptor sites of Tashkent in Uzbekistan, Khujand in Tajikistan and Turkmenabat in Turkmenistan are also shown.



and Khujand at around 09:00 UTC, 11:00 UTC and 12:00 UTC, respectively. Terra-MODIS true-colour observations and SEVIRI RGB images corroborate detection of a very thick dust plume. However, the intensity of the pink/magenta colours associated with dust in RGB imagery does not absolutely agree with the dust intensity, since the RGB signal could be affected by dust mineralogy, low-temperature inversions and dust-layer height (Brindley *et al.*, 2012; Solomos *et al.*, 2018). The extensive cloudiness over the mountainous ranges is detected in ochre and brown colors in RGB imagery. Note also the change in the desert-surface reflectance colour from light cyan during the early morning hours to yellow, light orange during noon and early afternoon hours on 4 November (Fig. 3).

3.2 Atmospheric Dynamics during the Dust Storm

This section analyses the atmospheric circulation patterns in the upper, middle, and lower troposphere during a 6-day period (1–6 November 2021) around the dust storm day (4 November 2021), aiming to reveal the dynamic conditions that were associated with the genesis, expansion and dissipation of the dust storm (Figs. 4–7). Prior to the dust storm, on 1 November, a typical cold atmospheric circulation formed over eastern Europe and the Balkan Peninsula, detected by a deep trough, which started to dissipate on 3 November (Fig. 4(a–c)). In the upper troposphere, these conditions were characterized by two relatively weak polar and subtropical jet streams over Russia and south Asia, respectively. The polar jet stream was progressively moving from central-west Siberia to east Kazakhstan, while marginal changes were observed in the sub-tropical jet stream, with a core of above 45 m s^{-1} over the Ganges valley and the Himalayas (Fig. 5(a–c)). The dynamic conditions created subsidence behind the subtropical jet core over the east of Iran, Afghanistan and Pakistan, while negative omega values at 300 hPa dominated over the Kazakhstan-Russia border, associated with the polar jet (Figs. 5(a–c)). In the meanwhile, the cold Siberian anticyclone was dominant over eastern Siberia, creating a strong gradient of geopotential heights across the Russia-Kazakhstan border. A high-pressure ridge prevailed on days prior to dust storm stretching from the Middle East and Iran to the Caspian Sea and western Russia, carrying warmer air masses over the region. These conditions created an omega blocking system over CA and Russia on days prior to the dust storm, while the axis of this ridge progressively shifted from southeast-to-northwest (1 November) to southwest-northeast on 4 November (Fig. 4), thus changing the upper-troposphere circulation. The upper-level conditions accompanied by stretching a trough in mid troposphere (500 hPa) over the northern borders of Kazakhstan, increased the instability along troposphere, which was induced to penetrate cold air masses from the Siberian region into CA. On 3 November, just prior to the dust storm, the polar jet, with a core of $35\text{--}45 \text{ m s}^{-1}$, moved from south Russia to east Kazakhstan, causing negative omega at 300 hPa over the region (Figs. 5(a–c)). These conditions maximized air subsidence over the Kazakhstan-Russia border, which was accompanied by the eastward replacement of the polar jet with air upward motion over southeast Kazakhstan (Fig. 5(c)). The circulation at 500 hPa level featured a typical omega blocking pattern, with a large ridge over west Russia and two troughs to its west and east, whereas the latter was much deeper than the former extending into the whole territory of Kazakhstan. A strong surface-temperature gradient was created along north Kazakhstan, with the minimum temperature below -30°C , which was moving northwards affecting the central-eastern part of Kazakhstan on 3–4 November, with characteristics of a cold front associated with the Siberian anticyclone. Furthermore, the establishment of the polar jet stream strengthened the vertical instability, helping the convergence and invasion of cold air mass into east Kazakhstan.

The atmospheric circulation on 4 November had a notable difference from that on 3 November, mostly detected by the strengthening of the jet stream over eastern Kazakhstan (wind speeds above 45 m s^{-1}). This jet stream was expanded over a much lower area, which was affected by an intensified trough, as a tongue of cold-air intrusion from the Siberian anticyclone (Figs. 4(d) and 5(d)). These meteorological conditions triggered highest negative omega values highlighted an upward air motion in the upper troposphere over east Kazakhstan and surroundings and is likely to be highly associated with the dust storm outbreak, as also shown in previous studies over the Middle East and the Mediterranean (Kaskaoutis *et al.*, 2019; Hamzeh *et al.*, 2021). These dynamic conditions also induced an intense gradient between northern divergence and southern convergence in Central Asia. Furthermore, in the middle troposphere (500 hPa), the south-westward trough

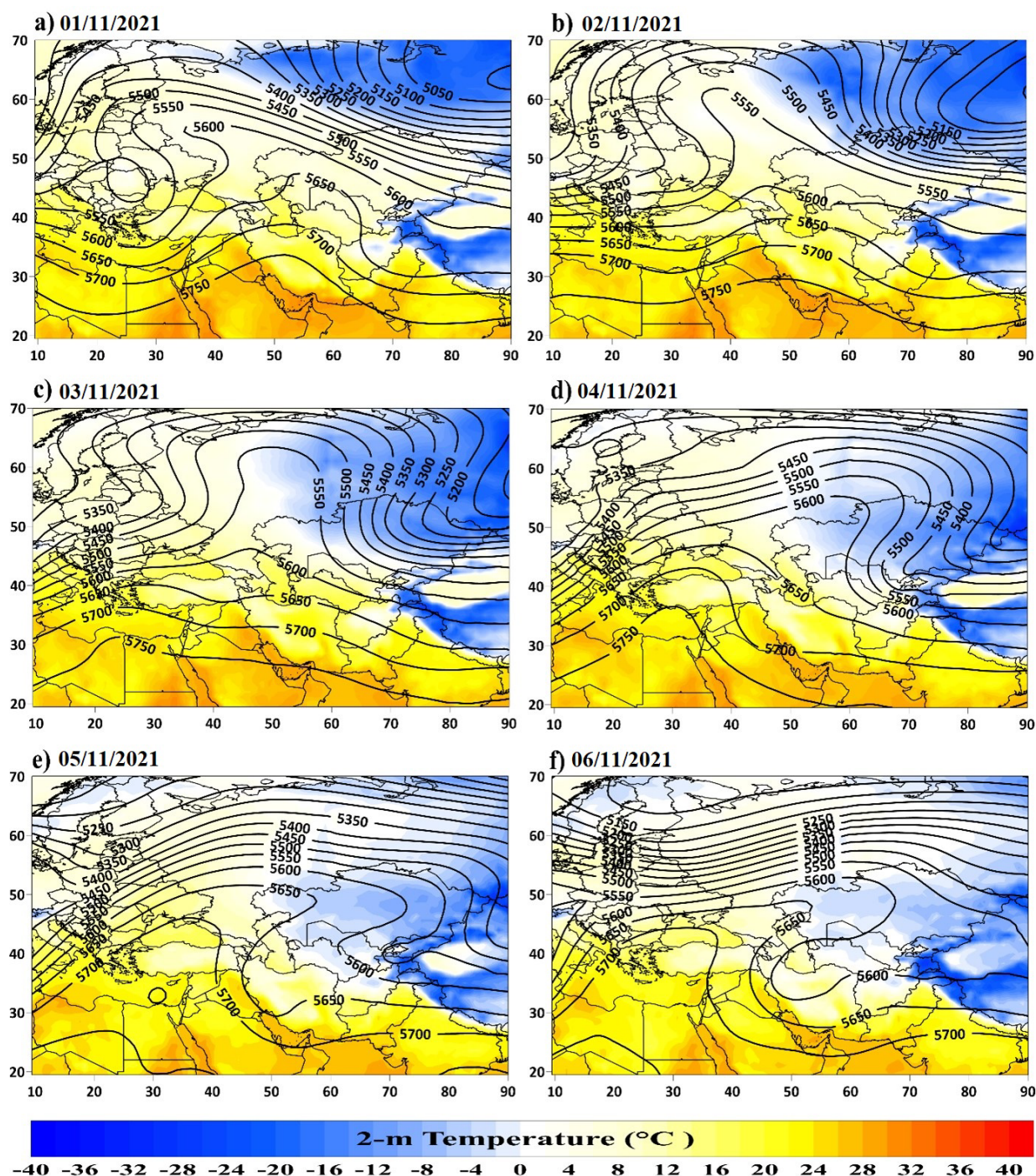
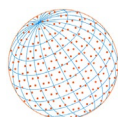


Fig. 4. (a–f) Composite maps of geopotential heights at 500 hPa (black contours) and surface temperature (shaded area) from 1 to 6 November 2021.

became deeper compared to previous day and it is stretched from Siberia to Iran, with the expanded ridge north-eastward, covering central Russia (Fig. 4(d)). The omega blocking system, accompanied with the Siberian anticyclone and favoured by the establishment of the upper-level jet stream over east Kazakhstan, seem to play a major role in the dust storm outbreak in east Kazakhstan. Although the atmospheric circulation patterns during intense dust storms in CA have not been well documented, being also variable depending on season and dust event (Kaskaoutis *et al.*, 2019; Tositti *et al.*, 2022), the role of the Siberian anticyclone, the position and movement of the upper-level jet stream seem to be very important factors controlling dust activity over CA during the cold period of the year.

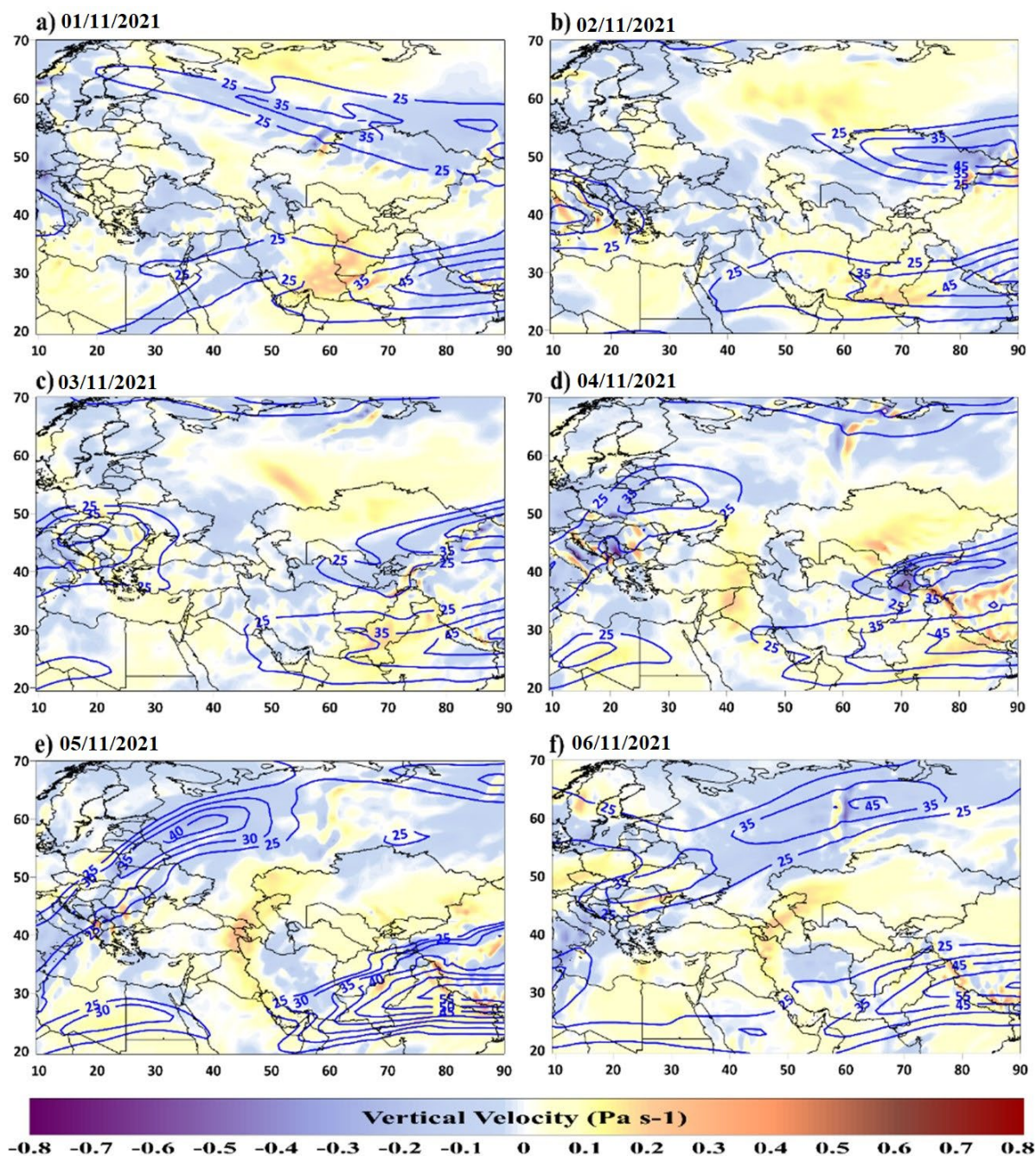
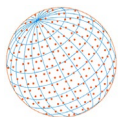
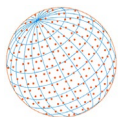


Fig. 5. (a–f) Composite maps of omega at 300 hPa (shaded area) and zonal wind at 250 hPa (blue contours) from 1 to 6 November 2021.

On 5 November, the strong zonal winds at 250 hPa ($> 25 \text{ m s}^{-1}$) covered an extended area from Italy toward western Russia (Fig. 5(e)), which was further extended to Siberia on the next day, while the upper-level jet over eastern Kazakhstan was dissipated and moved further to the south, practically merged with the subtropical upper-level jet over north India and the Tibetan Plateau (Fig. 5(f)). This weather pattern reflects rather stable upper-troposphere conditions accompanied by descending air, with positive omega values, over nearly the whole CA. The negative omega values prevailed in the northern edge of the subtropical jet (Fig. 5(e)), became more active air ascending over the trough-affected areas contributing to suction of cold air masses toward Tajikistan and northeast Pakistan on 5 November, when an expanded trough tongue covered the southeast Central Asian countries, extended over Iran (Fig. 4(e)). The omega blocking system over CA was significantly dissipated after the dust storm day and was limited to southern latitudes, as



a ridge over the East Mediterranean-Middle East (EMME) region. These conditions limited invasion of polar cold air and transferred warmer air masses over CA and pushed the trough toward the east, while a zonal circulation was established at northern latitudes over Russia (Figs. 4(e, f)).

The relative positions and intensity of the low- and high-pressure systems accompanied by the polar and subtropical jet streams at upper-levels, generally control the intensity of the surface regional winds and dust outbreaks (Mohammadpour *et al.*, 2022). The meteorological conditions due to Caspian's ridge at 500 hPa level facilitated the formation of high-pressure conditions at lower troposphere and at the surface over CA countries (Fig. 6). These conditions seem to modulate the dust activity over the region (Kaskaoutis *et al.*, 2016; Shi *et al.*, 2019). The dynamic pressure pattern on 2 November, which was a combination of two weak high-pressure systems

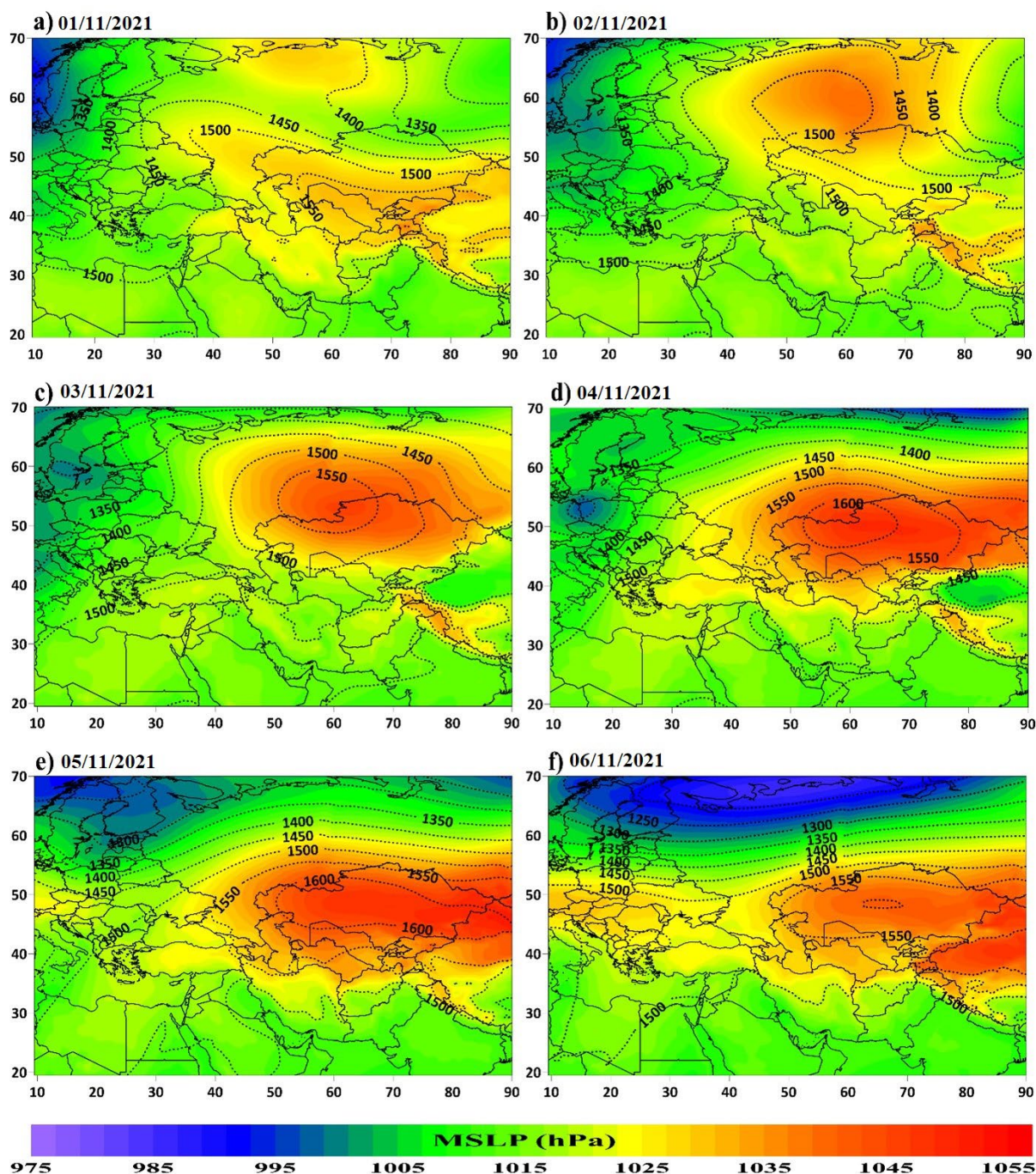
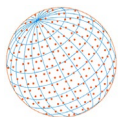


Fig. 6. (a–f) Composite maps of geopotential heights at 850 hPa (dash black contours) and mean sea-level pressure (MSLP, shaded area) from 1 to 6 November 2021.



over north Russia and CA on previous day, was characteristic of the omega blocking at the lower troposphere (850 hPa) and at the surface, with high-pressure conditions over central Siberia. The geopotential heights at 850 hPa presented even higher values on the next days (3 and 4 November 2021), with closed high-pressure systems over Kazakhstan, while at surface, high-pressure conditions of above 1040 hPa dominated over the whole Kazakhstan territory. The synoptic meteorology over the examined domain clearly dominated by this high-pressure system over CA, while lower pressure conditions prevailed in south Asia, the EMM region and in central/western Europe (Figs. 6(a–d)). This intense and expanded high-pressure system over CA (> 1600 gpm; > 1040 hPa over Kazakhstan), was a triggering dynamic for the formation of dust storm on 4 November 2021, while on the days after the dust storm, the core of the high-pressure system at 850 hPa was expanded over a larger area, slightly moved towards the east, and then significantly dissipated (Figs. 6(e–f)). These meteorological conditions were different from those usually prevailed during dust storms over southwestern CA in spring and summer that were attributed to high-pressure system over the Caspian Sea and thermal low-pressure over topographic-low areas in southern latitudes (Cheng *et al.*, 2019; Li *et al.*, 2019; Mohammadpour *et al.*, 2022). Overall, MSLP dynamics highly controlled the wind regime on days prior, during and after the intense dust storm of 4 November 2021 over southeastern Kazakhstan.

Fig. 6 shows the vector wind at the surface along with the spatial distribution of dust loading (in g m^{-2}) obtained from MERRA-2 over Central Asia from 1 to 6 November 2021. The establishment of the high-pressure system over the northern part of CA on 2 November, modified the wind regime from the previous day, with a strong anticyclonic flow over Kazakhstan, which further intensified on 3 November. The easterly winds, propagated from the southern flanks of the high-pressure system over the southern part of CA, passed over Moynkum, eastern Kyzylkum, Aralkum and Karakum Deserts (Zhou *et al.*, 2019) and advected high dust loading covering a wide area till the shores of the Caspian Sea (Figs. 7(b–c)). At the same time, winter Shamal wind facilitated increased dust loading over the Syrian–Iraqi plains. A strong northerly/north-easterly flow dominated over the dust-source area, as well as over the alluvial dried beds in the Balkhash basin in east Kazakhstan, favouring dust emissions. On the dust storm day (4 November 2021), the associated changes in the distribution of G850, MSLP and wind regimes over the central Asian countries, indicated that the strengthened high-pressure system intensified the dominant anticyclonic wind pattern compared to previous days. The prevailing surface wind propagated from the southern Balkhash basin blowing toward the Caspian Sea and affected the southern half of Kazakhstan and nearly whole territories of Uzbekistan and Turkmenistan (Fig. 7(d)). These areas are covered by high columnar dust loading greater than 1.1 g m^{-2} , probably emitted from the various deserts such as Aralkum, Kyzylkum, Trans-Unguz, and central Karakum and alluvial dried beds of the Caspian lowlands (Nobakht *et al.*, 2021). Therefore, apart from the thick dust plume that covered the Tashkent area on 4 November 2021 and caused several socio-economic and health impacts on local population, the north-easterly/easterly flows generated from the centre of the anticyclone over Kazakhstan facilitated an extensive dust blanket over the southern parts of CA, also covering the Caspian Sea (Fig. 7(d)). The synoptic conditions on 5 November presented large similarities with the dust storm day, and this is also shown in the vector wind pattern, while the dust loading was progressively dissipated with lower values (~ 0.5 to 0.7 g m^{-2}) over southern CA (Fig. 7(e)). MERRA-2 observations show high dust loading over the Tarim Basin and Taklimakan Desert, likely caused by convergence of winds over these desert areas and a significant dust transport from Libya towards south Italy and the Balkans due to strong southerlies. On the next day, 6 November 2021 (Fig. 7(f)), the dust loading over Central Asia was further reduced, while the dust hotspots over Taklimakan, central Mediterranean and the Indo-Gangetic plains intensified.

3.3 Ground-based Meteorological Observations

PM_{2.5} concentrations in Tashkent

Fig. 8 shows the variation of hourly PM_{2.5} concentrations from the air quality station located in the US embassy in Tashkent, Uzbekistan from 1 to 10 November 2021. The PM_{2.5} concentrations are color-coded with the Air Quality Index (AQI) data classified for the six AQI categories (good, satisfactory, moderate, poor, very poor and severe) related to various health clusters for the local

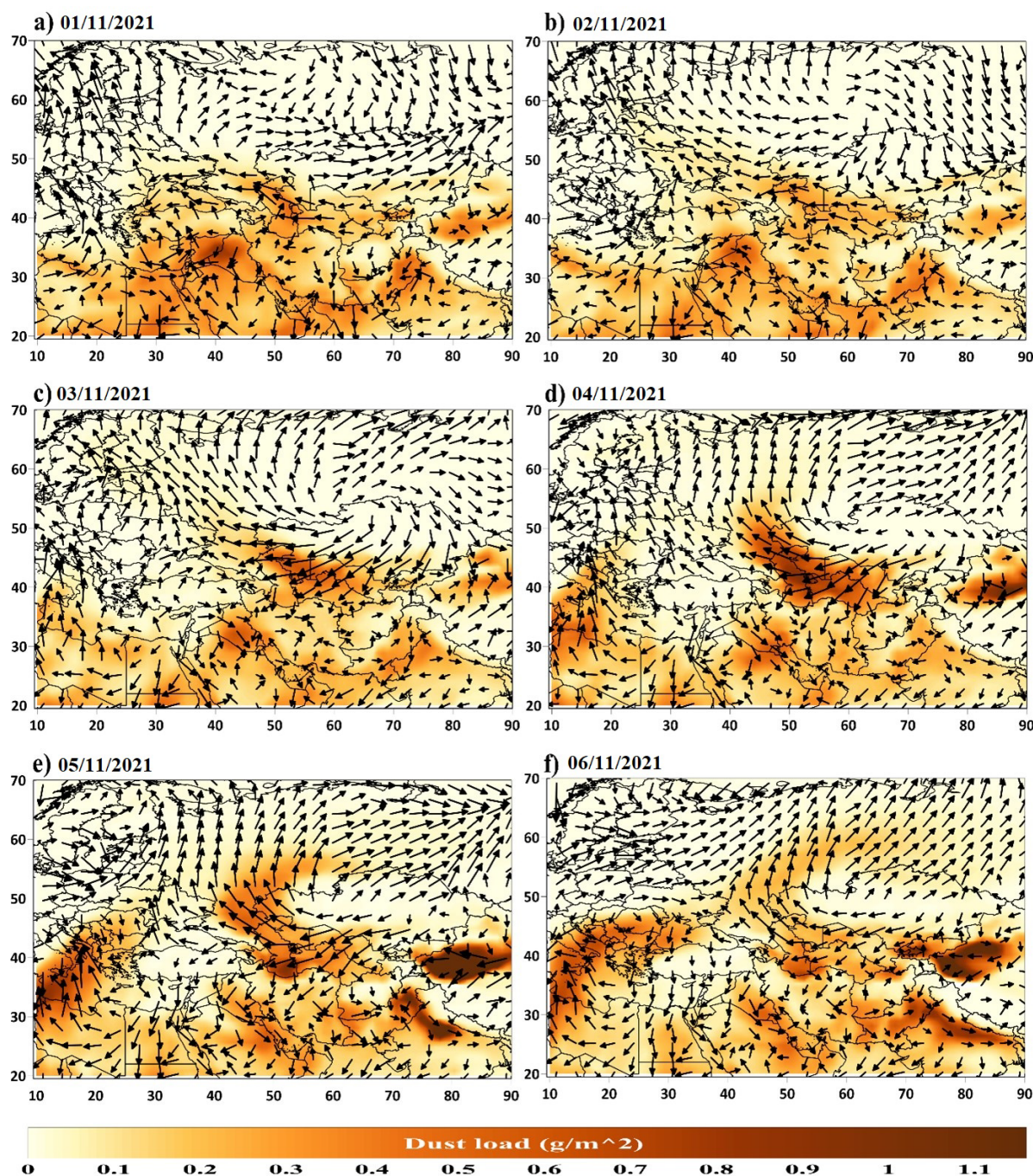
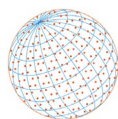


Fig. 7. (a–f) Composite maps of dust load (g m^{-2}) and surface vector winds (m s^{-1}) from 1 to 6 November 2021.

population (from good to hazardous). Around 18:00 pm on 4 November 2021, there was a spike in $\text{PM}_{2.5}$ levels caused by the arrival of the severe dust storm originated from southeast Kazakhstan. $\text{PM}_{2.5}$ concentrations raised above $900 \mu\text{g m}^{-3}$ during the afternoon hours on 5 November. On 5 and 6 November, the AQI values were categorized in the very unhealthy and hazardous class for any group of population in Tashkent. There was a gap in $\text{PM}_{2.5}$ recordings between 22:00 pm on 4 November and 17:00 pm on 5 November, probably attributable to instrument failure caused by the severe PM concentrations. The daily mean $\text{PM}_{2.5}$ concentrations were $393 \mu\text{g m}^{-3}$ (26 times higher than the guideline level of $15 \mu\text{g m}^{-3}$ according to WHO), $215 \mu\text{g m}^{-3}$ (14 times higher) and $111 \mu\text{g m}^{-3}$ (7.5 times higher), on 6, 7 and 8 November, respectively (WHO, 2021). The intense dust haze (caused by particles raised into the atmosphere by a recent dust or sand storm) started dissipating in the evening hours of 6 November. Still, dust particles remained till about 15 November

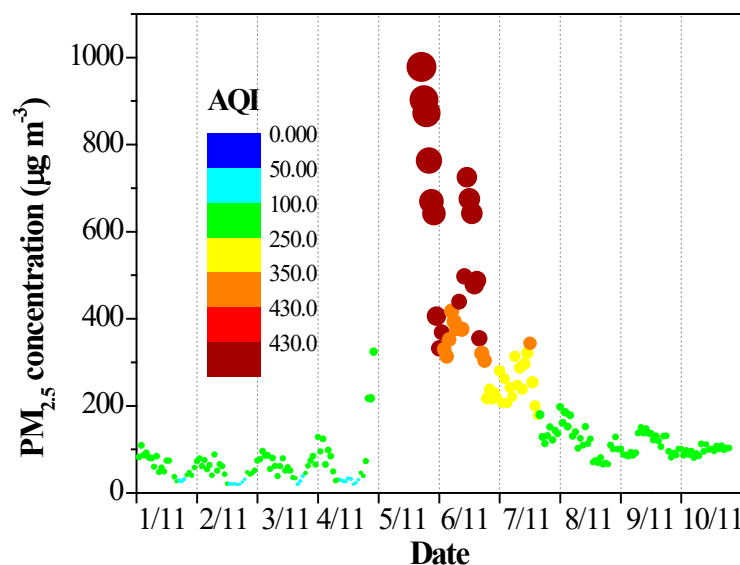
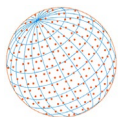


Fig. 8. Hourly $\text{PM}_{2.5}$ concentrations in Tashkent around the dust storm day (4 November 2021), color-coded with the AQI values.

when heavy rain helped to wet deposition of PM. Similarly elevated $\text{PM}_{2.5}$ concentrations during severe dust storms have been reported in other parts of the world (Dumka *et al.*, 2019; Hussein *et al.*, 2020; Wu *et al.*, 2021). In Beijing, China, Wu *et al.* (2021) reported daily mean $\text{PM}_{2.5}$ concentrations exceeding $200 \mu\text{g m}^{-3}$ on 15 March 2021 caused by an intense dust storm originating in Mongolia. In addition, $\text{PM}_{2.5}$ levels were $\sim 109 \mu\text{g m}^{-3}$ on 25 July 2018 in Amman, Jordan during a dust storm episode originating in the Sahara Desert (Hussein *et al.*, 2020; Shafiee *et al.*, 2017; Niroomand *et al.*, 2020).

3.3.1 Changes in horizontal visibility and 10-m wind speed

Fig. 9 shows the hourly ground-based measurements of horizontal visibility and wind speed during 1–6 November 2021 at three sites in CA (Turkmenabat, Tashkent and Khujand) directly affected by the dust storm. In Turkmenabat, the dust arrived at around 09:00 UTC on 4 November and lasted for approximately 15 hours. During the arrival of the dust storm, visibility dropped drastically from about 10 km to 1 km, accompanied by a notable increase of wind speed from about 4 m s^{-1} to $10\text{--}12 \text{ m s}^{-1}$ during the peak of the dust storm over the site (Fig. 8(a)). The minimum horizontal visibility was recorded at 15:00 UTC with a value of 692 m, when the wind speed was 12.5 m s^{-1} .

In Tashkent, horizontal visibility varied considerably on days prior to the dust storm, while the large gaps in visibility were accompanied by weak-to-calm winds ($< 1\text{--}2 \text{ m s}^{-1}$) that favoured the accumulation of anthropogenic aerosols and pollutants near the ground. This is a characteristic atmospheric condition in urban-polluted environments, where the weak winds and temperature inversions are responsible for trapping aerosols near the ground, which contribute to scattering of solar radiation and visibility degradation (Dumka *et al.*, 2017; Liakakou *et al.*, 2020). However, on 4 November the dramatic decrease in visibility was accompanied by a notable increase in wind speed ($6\text{--}7 \text{ m s}^{-1}$) signalling the arrival of the dust storm (Fig. 9(b)). As mentioned above, Tashkent was severely affected by this severe dust storm, which reduced visibility below 1000 m at 15:00 UTC and below 200 m between 16:00–18:00 UTC (4 November 2021). Dust aerosols over the city remained for the next 8 days, contributing to the reduced visibility ($< 2\text{--}3 \text{ km}$; Fig. 9(b)) and the increased $\text{PM}_{2.5}$ concentrations compared to pre dust storm days.

In Khujand, the dust plume arrived at 12:00 UTC and immediately caused a reduction in visibility to below 2.5 km. As the dust plume thickened, visibility dropped below 1 km for about 7 hours. At the time of dust arrival, the wind speed in Khujand was 10 m s^{-1} , while the changes in wind speed and visibility due to arrival of the dust storm were mostly similar in all the examined stations. This indicated that the thick dust plume that blanketed these sites was approaching in

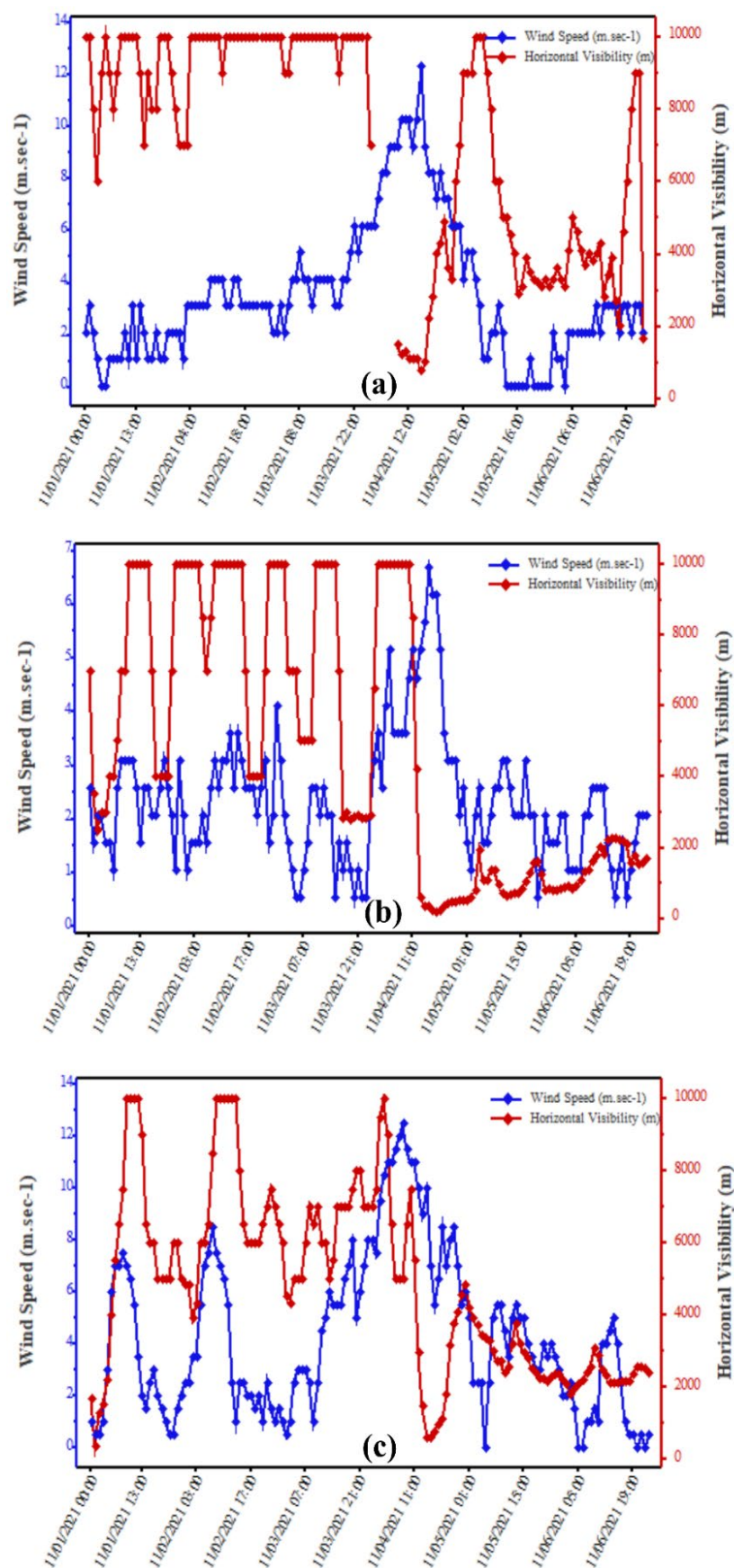
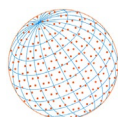
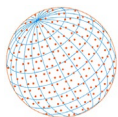


Fig. 9. Hourly ground-based measurements of wind speed and horizontal visibility at stations in Central Asia, (a) Turkmenabat, (b) Tashkent and (c) Khujand during 1-6 November 2021.



the form of a dust wall accompanied by strong near-surface winds, resulting in a strong negative correlation between wind speed and horizontal visibility. On the days prior to the dust storm, visibility records were mostly affected by local activities in the cities, while on the days after the dust storm, the visibility remained at general low levels, until atmospheric cleaning.

3.3.2 Variations in surface air-temperature

Fig. 10 shows the temperature variation during the first half of November 2021 in Tashkent, Khujand, and Turkmenabat. The data showed that the dust intrusion on 4 November significantly changed the temperature regime in the region. As mentioned above, dust particles remained in the atmosphere for a long time, until heavy rain cleaned the air on 15 November 2021 in Tashkent and Khujand. In Turkmenabat, there was no rain, but horizontal visibility started to increase above 10 km from 14 November 2021, after the removal of dust aerosols.

In Turkmenabat, the daytime air temperature decreased on 4 November 2021 compared to 3 November 2021 (before dust event) and 11 November 2021 (after dust event) by -11.8°C and -3.4°C , respectively. However, opposite changes in nighttime temperature occurred by $+5.1^{\circ}\text{C}$ and $+10.4^{\circ}\text{C}$ relative to the days before and after the dust event. A similar situation was observed in Tashkent, where the daytime temperature decreased by -9.8°C and -10.1°C relative to 2 November 2021 and 12 November 2021, while at night there was an increase in temperature by $+2.3^{\circ}\text{C}$ and $+2.9^{\circ}\text{C}$, respectively. In Khujand, the dust storm on 4 November 2021, caused a notable decrease in daytime air temperature by -8.6°C and -12.5°C with respect to 2 and 13 November 2021. The respective nighttime air temperatures were higher on 4 November by $+9.5^{\circ}\text{C}$ and $+8.4^{\circ}\text{C}$ compared to aforementioned days. It should be noted that apart from the aforementioned temperature amplitudes between the dust day and specific days before and after the dust event, the arrival of the dust storm over each station caused a notable decrease in air temperature (Fig. 10), which is partly attributed to presence of a cold front associated with dust and to radiative impact of dust on solar radiation.

Similar temperature changes with the arrival of intense dust storms have been reported at several sites worldwide (Alharbi *et al.*, 2013; Kaskaoutis *et al.*, 2019; Maghrabi *et al.*, 2011; Prakash *et al.*, 2015). Kaskaoutis *et al.* (2019) reported a considerable decrease in maximum temperature ($\sim 8\text{--}11^{\circ}\text{C}$) due to dust radiative cooling and the passage of a cold front on 5–6 February 2019 compared to 4 February 2019 in Zabol, Iran. The Middle East also experienced a remarkable reduction of -6.7°C in temperature due to the dust radiative cooling during severe dust storms from 18 to 22 March 2012 (Prakash *et al.*, 2015). According to previous studies, mineral dust particles have an important role in global energy balance via both direct (on solar radiation) and indirect (on clouds) effects (Kok *et al.*, 2018, 2017). Generally, when shortwave radiation encounters dust aerosols, cooling happens because some radiation does not reach the Earth's surface. On the other hand, dust particles can also absorb longwave radiation, emitted by the earth, atmosphere and clouds, and contributes to planetary warming (Kok *et al.*, 2018; Mahowald *et al.*, 2014; Miller *et al.*, 2006; Tegen and Lacis, 1996).

3.4 Backward Trajectory Analysis

To monitor the movement of the dust storm that affected the three receptor sites, the HYSPLIT-4 model was implemented to analyse the transport pathway of dust particles through 3-hour time intervals up to 48 hours before dust episodes reaching the study locations (Fig. 11). The starting point of trajectories was in Turkmenabat on 4/11/2021 at 09:00 UTC, in Tashkent on 4/11/2021 at 11:00 UTC, and in Khujand on 4/11/2021 at 12:00 UTC. The arriving height of the air masses at the receptor sites was set at mid boundary layer height to guarantee both transition and ending of dust trajectories in the boundary layer (Broomandi *et al.*, 2021; Karaca *et al.*, 2009).

Turkmenabat, in central Turkmenistan, was hit by the dust plume on 4 November at 09:00 UTC, while the air masses at the altitude of 275 m originated from north/north-eastern directions, i.e., Qaraghandy and Pavlodar in Kazakhstan (Fig. 11(a)), passing over southeast Kazakhstan, where the dust storm was generated (Fig. 2(b)). Similar air mass pathways are observed in Tashkent (Fig. 11(b)), which was upwind of the dusty air masses that hit Turkmenabat. The starting points of the majority of the air masses at 130 m altitude (mid-boundary layer height) were from eastern and central Kazakhstan, and continued to the Almaty region, Jambyl and south Kazakhstan,

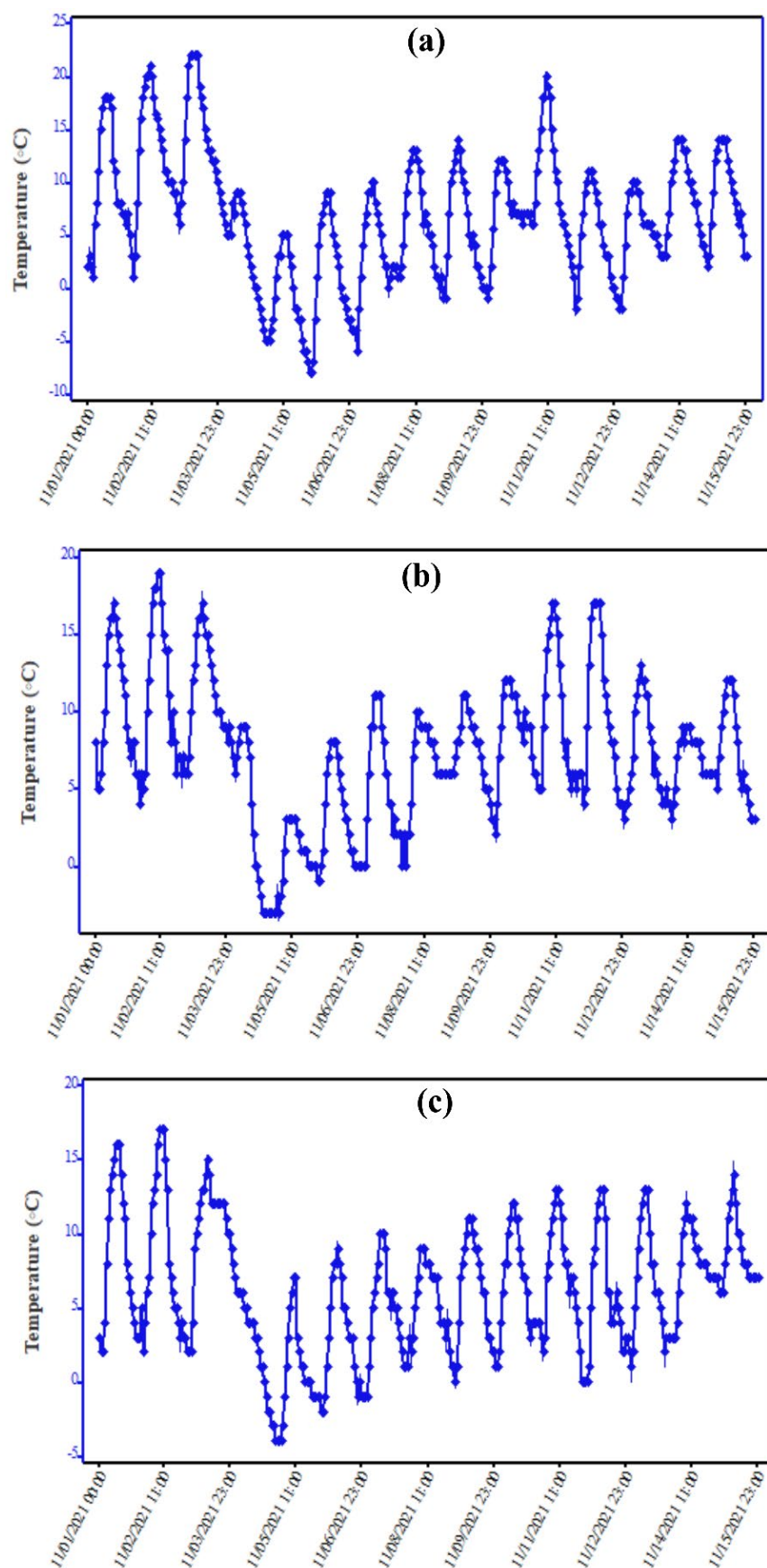
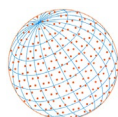


Fig. 10. The hourly ground-based measurements (2-m temperature) for the study stations of (a) Turkmenabat, (b) Tashkent, and (c) Khujand between 1–15 November 2021.

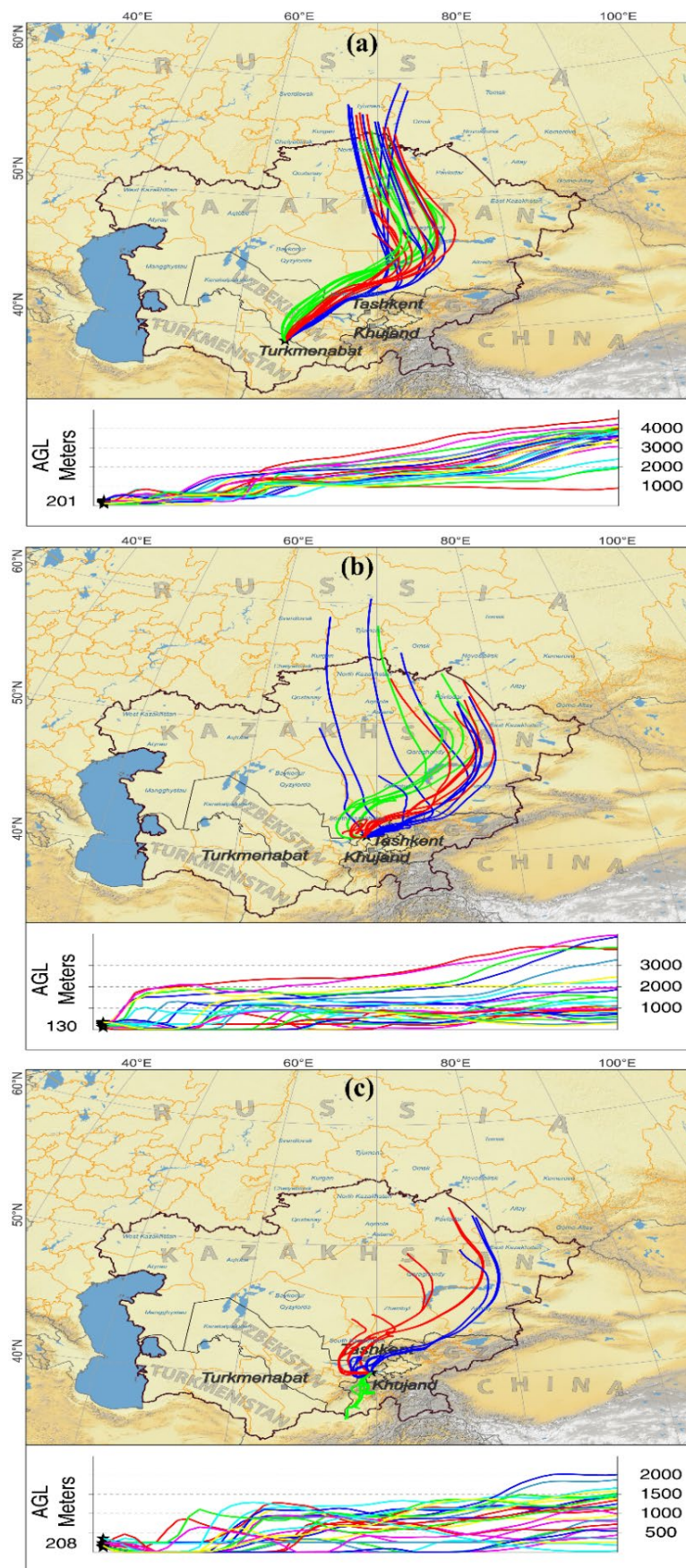
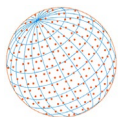
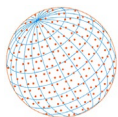


Fig. 11. Backward trajectory analysis by HYSPLIT model at receptor sites of (a) Turkmenabat, (b) Tashkent, and (c) Khujand on 4 November 2021 (the dust storm day).



before reaching Tashkent (Fig. 11(b)). The dusty air masses that hit Khujand travelled over the same regions (Fig. 11(c)), while the results of trajectories simulation were consistent with the SEVIRI Visible/IR imagery (Fig. 3) during the dust intrusion, indicating that air masses were mainly originated from south-western parts of Russia, as well as eastern, central, and southern Kazakhstan. While they were passing over dust sources located in south Kazakhstan, including Kyzylorda and Kyzylkum Deserts, the transport of dust particles was facilitated by the northeast winds toward Turkmenabat, Khujand and Tashkent in the afternoon of 4 November 2021.

3.5 Land Degradation in Central Asia and Future Projections

The 4 November severe dust storm over south-eastern Kazakhstan that affected a large area in CA, was a unique and rare phenomenon, in terms of its intensity, that happened in an area vulnerable to dust emissions and with continuous soil degradation during recent decades due to ongoing human interventions (Aiman *et al.*, 2018; Baubekova *et al.*, 2021; Guney *et al.*, 2021; Kismelyeva *et al.*, 2021; Ramazanova *et al.*, 2021). Apart from the high PM concentrations during dust storms, potentially toxic elements (PTEs) as soil contaminants transported by dust may add more health and ecological concerns over the CA region.

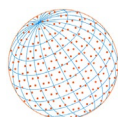
Due to the potentially toxic-contaminated soils in arid areas of CA, it is recommended to perform site-specific studies, also examining the chemical composition during intense dust storms. It is also highly recommended to take effective and immediate stabilising measures to control the wind erosion in vulnerable areas. Since sand and dust storm (SDS) activity is an alarming challenge to sustainable development in more than 150 countries that are directly affected by SDS worldwide (Middleton and Kang, 2017), it is necessary to prepare suitable climate adaptation and mitigation strategies, developing more reliable and accurate early warning systems and quantifying the impacts to societal implications in both national and regional scales. A transboundary multi-hazard risk assessment is also essential in analysing the cause-and-effect relationships and helping policymakers to fully understand the required dynamics and complexity of policy actions. Such transboundary dialogue and collaboration between the affected countries lead to policy interventions reflecting the geospatial link among the origins and receptors, which can positively influence both adaption and mitigation aspects.

4 CONCLUSIONS

This study investigated a severe dust storm that occurred on 4 November 2021 over Central Asia, a phenomenon unprecedented in this region over the last 150 years (Eurasianet, 2021) that caused an increase of PM₁₀ concentrations above 18,000 $\mu\text{g m}^{-3}$ in Tashkent, Uzbekistan. Meteorological measurements at selected sites in Central Asia including Turkmenabat in Turkmenistan, Khujand in Tajikistan and Tashkent in Uzbekistan showed that a large part of Central Asia was highly impacted by this unique dust storm, which reduced horizontal visibility to 200–1000 m and daytime temperature by 2–4°C at different time periods. The thick dust plume that blanketed these sites approached in the form of a dust wall accompanied by strong near-surface winds.

Favourable meteorological conditions for the formation of an intense dust storm prevailed both in the upper and lower troposphere over Central Asia and more specifically over the eastern Kazakhstan, which was detected by SEVIRI imagery as the main dust-source region. A high-pressure ridge prevailed during the day prior to the dust storm, stretching from the Middle East and Iran to the Caspian Sea and west Russia, creating a typical omega blocking pattern at 500 hPa level, with a large ridge over west Russia and two troughs to its west and east. The axis of the ridge progressively shifted from southeast-to-northwest (1 November) to southwest-northeast on 4 November, resulting in a strong surface air-temperature gradient and invasion of cold air masses associated with the anticyclonic system over Kazakhstan. The intense high-pressure system over CA was a triggering dynamic force for the formation of the dust storm on 4 November 2021, due to strong easterly winds from the southern flanks of the high-pressure system toward the southern part of CA, passing over Aralkum, Moynkum, Kyzylorda, eastern Kyzylkum, Trans-Unguz, and central Karakum Deserts. On the dust storm day, an intense jet stream with core wind values of about 4 m s⁻¹ was located just above the dust-source region in southeastern Kazakhstan.

HYSPLIT air-mass back trajectories at the receptor sites of Turkmenabat, Khujand, and Tashkent



were consistent with SEVIRI satellite data regarding the apportionment of the dust intrusions at each site, indicating that the dusty air masses mainly originated from the south-eastern parts of Kazakhstan, including Kyzylorda and Kyzylkum Deserts. The transport of dust plumes was facilitated by the northeast winds toward Turkmenabat, Khujand, and Tashkent in the afternoon of 4 November 2021. Central Asia is considered a highly sensitive area in view of climate change due to projections of precipitation decrease and increased possibility of prolonged droughts. Under such climatic conditions in the future, severe dust storms in the area will inevitably follow an increasing frequency, causing large deterioration to atmospheric environment and major socio-economic issues in the countries of Central Asia.

ACKNOWLEDGMENTS

The authors acknowledge the financial support for the NU projects (Nazarbayev Research Fund SOE2017003 & 11022021CRP1512). Kawe | Kaveh M. acknowledges grant support by Iran National Science Foundation (INSF) under post-doctoral project No. 4001142. A.R acknowledges support by Iran National Science Foundation (INSF) under project No 99003984. The authors thank Earth data, NASA, the ECMWF and Copernicus teams for providing the MODIS, MERRA-2 and ERA-5 products used in this work.

ADDITIONAL INFORMATION AND DECLARATIONS

Conflict of Interest

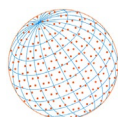
The authors declare that they have no conflict of interest.

Credit Authorship Contribution Statement

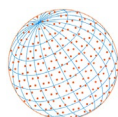
Parya Broomandi: Conceptualization, Methodology, Software, Data Curation, Formal Analysis, Validation, Investigation, Visualization, Writing - Original Draft. **Kaveh Mohammadpour:** Conceptualization, Methodology, Software, Data Curation, Formal Analysis, Validation, Investigation, Visualization, Writing - Original Draft. **Dimitris G. Kaskaoutis:** Conceptualization, Methodology, Validation, Writing - Review & Editing. **Sabur F. Abdullaev:** Formal Analysis, Data Curation, Resources. **Vladimir A. Maslov:** Formal Analysis, Data Curation, Resources. **Amirhossein Nikfal:** Data Curation, Software. **Aram Fathian:** Data Curation, Software. **Ali Jahanbakhshi:** Data Curation, Software. **Bakhyt Aubakirova:** Data Curation. **Jong Ryeol Kim:** Funding acquisition, Project administration Resources. **Alfredo Satyanaga:** Funding acquisition, Project administration, Resources. **Alireza Rashki:** Formal Analysis, Visualization. **Nick Middleton:** Original concept, Supervision, Validation, Writing - Review & Editing.

REFERENCES

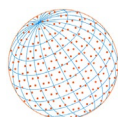
- Achilleos, S., Al-Ozairi, E., Alahmad, B., Garshick, E., Neophytou, A.M., Bouhamra, W., Yassin, M.F., Koutrakis, P. (2019). Acute effects of air pollution on mortality: A 17-year analysis in Kuwait. *Environ. Int.* 126, 476–483. <https://doi.org/10.1016/j.envint.2019.01.072>
- Aghababaeian, H., Ostadtaghizadeh, A., Ardalan, A., Asgary, A., Akbary, M., Yekaninejad, M.S., Stephens, C. (2021). Global health impacts of dust storms: A systematic review. *Environ. Health Insights* 15, 11786302211018390. <https://doi.org/10.1177/11786302211018390>
- Aili, A., Kim Oanh, N.T. (2015). Effects of dust storm on public health in desert fringe area: Case study of northeast edge of Taklimakan Desert, China. *Atmos. Pollut. Res.* 6, 805–814. <https://doi.org/10.5094/APR.2015.089>
- Aiman, N., Gulnaz, S., Alena, M. (2018). The characteristics of pollution in the big industrial cities of Kazakhstan by the example of Almaty. *J. Environ. Heal. Sci. Eng.* 16, 81–88. <https://doi.org/10.1007/s40201-018-0299-1>
- Aleya, L., Uddin, M.S. (2020). Environmental pollutants and the risk of neurological disorders. *Environ. Sci. Pollut. Res.* 27, 44657–44658. <https://doi.org/10.1007/s11356-020-11272-3>
- Alharbi, B., Maghrabi, A., Tapper, N. (2013). The March 2009 dust event in Saudi Arabia: Precursor



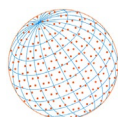
- and supportive environment. *Bull. Am. Meteorol. Soc.* 94, 515–528. <https://doi.org/10.1175/BAMS-D-11-00118.1>
- Al-Hemoud, A., Al-Dousari, A., Al-Shatti, A., Al-Khayat, A., Behbehani, W., Malak, M. (2018). Health impact assessment associated with exposure to PM₁₀ and dust storms in Kuwait. *Atmosphere* 9, 6. <https://doi.org/10.3390/atmos9010006>
- Almaganbetov, N., Grigoruk, V. (2008). Degradation of Soil in Kazakhstan: Problems and Challenges, in: Simeonov, L., Sargsyan, V. (Eds.), *Soil Chemical Pollution, Risk Assessment, Remediation and Security*, Springer Netherlands, Dordrecht, pp. 309–320. https://doi.org/10.1007/978-1-4020-8257-3_27
- Ashrafi, K., Shafiepour-Motlagh, M., Aslemand, A., Ghader, S. (2014). Dust storm simulation over Iran using HYSPLIT. *J. Environ. Health Sci. Eng.* 12, 9. <https://doi.org/10.1186/2052-336X-12-9>
- Baubekova, A., Akindykova, A., Mamirova, A., Dumat, C., Jurjanz, S. (2021). Evaluation of environmental contamination by toxic trace elements in Kazakhstan based on reviews of available scientific data. *Environ. Sci. Pollut. Res.* 28, 43315–43328. <https://doi.org/10.1007/s11356-021-14979-z>
- Booth, B.B.B., Dunstone, N.J., Halloran, P.R., Andrews, T., Bellouin, N. (2012). Aerosols implicated as a prime driver of twentieth-century North Atlantic climate variability. *Nature* 484, 228–232. <https://doi.org/10.1038/nature10946>
- Brindley, H., Knippertz, P., Ryder, C., Ashpole, I. (2012). A critical evaluation of the ability of the Spinning Enhanced Visible and Infrared Imager (SEVIRI) thermal infrared redgreen-blue rendering to identify dust events: Theoretical analysis. *J. Geophys. Res.* 117, D07201. <https://doi.org/10.1029/2011JD017326>
- Broomandi, P., Karaca, F., Guney, M., Fathian, A., Geng, X., Kim, J.R. (2021). Destinations frequently impacted by dust storms originating from southwest Iran. *Atmos. Res.* 248, 105264. <https://doi.org/10.1016/j.atmosres.2020.105264>
- Chen, T., Bao, A., Jiapaer, G., Guo, H., Zheng, G., Jiang, L., Chang, C., Tuerhanjiang, L. (2019). Disentangling the relative impacts of climate change and human activities on arid and semiarid grasslands in Central Asia during 1982–2015. *Sci. Total Environ.* 653, 1311–1325. <https://doi.org/10.1016/j.scitotenv.2018.11.058>
- Chin-Chan, M., Navarro-Yepes, J., Quintanilla-Vega, B. (2015). Environmental pollutants as risk factors for neurodegenerative disorders: Alzheimer and Parkinson diseases. *Front. Cell. Neurosci.* 9, 124. <https://doi.org/10.3389/fncel.2015.00124>
- Commission on Sustainable Development (CSD) (2002). Commission on Sustainable Development, UNDP, Country Profile Report, World Summit on Sustainable Development, Johannesburg. <https://sustainabledevelopment.un.org/csd.html>
- Creamean, J., Spackman, J., Davis, S., White, A. (2014). Climatology of long-range transported asian dust along the West Coast of the United States. *J. Geophys. Res.* 119, 12171–12185. <https://doi.org/10.1002/2014JD021694>
- Díaz, J., Linares, C., Carmona, R., Russo, A., Ortiz, C., Salvador, P., Trigo, R.M. (2017). Saharan dust intrusions in Spain: Health impacts and associated synoptic conditions. *Environ. Res.* 156, 455–467. <https://doi.org/10.1016/j.envres.2017.03.047>
- Dumka, U.C., Tiwari, S., Kaskaoutis, D.G., Hopke, P.K., Singh, J., Srivastava, A.K., Bisht, D.S., Attri, S.D., Tyagi, S., Misra, A., Pasha, G.S.M. (2017). Assessment of PM_{2.5} chemical compositions in Delhi: primary vs secondary emissions and contribution to light extinction coefficient and visibility degradation. *J. Atmos. Chem.* 74, 423–450. <https://doi.org/10.1007/s10874-016-9350-8>
- Dumka, U.C., Kaskaoutis, D.G., Francis, D., Chaboureaud, J.P., Rashki, A., Tiwari, S., Singh, S., Liakakou, E., Mihalopoulos, N. (2019). The role of the intertropical discontinuity region and the heat-low in dust emission and transport over the Thar desert - India: A pre-monsoon case study. *J. Geophys. Res.* 124, 13197–13219. <https://doi.org/10.1029/2019JD030836>
- Eurasianet (2021). Severe dust storm engulfs Uzbekistan. <https://eurasianet.org/severe-dust-storm-engulfs-uzbekistan>
- Galán-Madruga, D., Terroba, J.M., Dos Santos, S.G., Úbeda, R.M., García-Camero, J.P. (2020). Indoor and outdoor PM₁₀-bound PAHs in an urban environment. Similarity of mixtures and source attribution. *Bull. Environ. Contam. Toxicol.* 105, 951–957. <https://doi.org/10.1007/s00128-020-03047-w>
- Galán-Madruga, D. (2022). Urban air quality changes resulting from the lockdown period due to



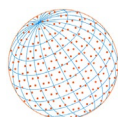
- the COVID-19 pandemic. *Int. J. Environ. Sci. Technol.* <https://doi.org/10.1007/s13762-022-04464-6>
- Galán-Madruga, D., García-Camero, J.P. (2022). An optimized approach for estimating benzene in ambient air within an air quality monitoring network. *J. Environ. Sci.* 111, 164–174. <https://doi.org/10.1016/j.jes.2021.03.005>
- Galán-Madruga, D., Ubeda, R.M., Terroba, J.M., Dos Santos, S.G., García-Camero, J.P. (2022). Influence of the products of biomass combustion processes on air quality and cancer risk assessment in rural environmental (Spain). *Environ. Geochem. Health* 44, 2595–2613. <https://doi.org/10.1007/s10653-021-01052-4>
- Gao, H., Washington, R. (2009). The spatial and temporal characteristics of TOMS AI over the Tarim Basin, China. *Atmos. Environ.* 43, 1106–1115. <https://doi.org/10.1016/j.atmosenv.2008.11.013>
- Global Environment Facility (GEF) (2003). Global Environment Facility, Operating Program on Sustainable Land Management # 15.
- Gelaro, R., McCarty, W., Suárez, M.J., Todling, R., Molod, A., Takacs, L., Randles, C.A., Darmenov, A., Bosilovich, M.G., Reichle, R. (2017). The modern-era retrospective analysis for research and applications, version 2 (MERRA-2). *J. Clim.* 30, 5419–5454. <https://doi.org/10.1175/JCLI-D-16-0758.1>
- Ghaisas, S., Maher, J., Kanthasamy, A. (2016). Gut microbiome in health and disease: Linking the microbiome-gut-brain axis and environmental factors in the pathogenesis of systemic and neurodegenerative diseases. *Pharmacol. Ther.* 158, 52–62. <https://doi.org/10.1016/j.pharmthera.2015.11.012>
- Gholami, H., Mohamadifar, A., Malakooti, H., Esmailpour, Y., Golzari, S., Mohammadi, F., Li, Y., Song, Y., Kaskaoutis, D., Fitzsimmons, K., Collins, A. (2021). Integrated modelling for mapping spatial sources of dust in central Asia - An important dust source in the global atmospheric system. *Atmos. Pollut. Res.* 12, 101173. <https://doi.org/10.1016/j.apr.2021.101173>
- Ginoux, P., Prospero, J.M., Torres, O., Chin, M. (2004). Long-term simulation of global dust distribution with the GOCART model: correlation with North Atlantic Oscillation. *Environ. Model. Softw.* 19, 113–128. [https://doi.org/10.1016/S1364-8152\(03\)00114-2](https://doi.org/10.1016/S1364-8152(03)00114-2)
- Gordeev, S.A., Posokhov, S.I., Kovrov, G.V., Katenko, S.V. (2013). Psychophysiological characteristics of panic disorder and generalized anxiety disorder. *Zhurnal Nevrol. i psikiatrii Im. S.S. Korsakova* 113, 11–14.
- Guney, M., Kumisbek, A., Akimzhanova, Z., Kismelyeva, S., Beisova, K., Zhakiyeva, A., Inglezakis, V., Karaca, F. (2021). Environmental partitioning, spatial distribution, and transport of atmospheric mercury (Hg) originating from a site of former chlor-alkali plant. *Atmosphere* 12, 275. <https://doi.org/10.3390/atmos12020275>
- Hamzeh, N.H., Karami, S., Kaskaoutis, D.G., Tegen, I., Moradi, M., Opp, C. (2021). Atmospheric dynamics and numerical simulations of six frontal dust storms in the Middle East region. *Atmosphere* 12, 125. <https://doi.org/10.3390/atmos12010125>
- Hashizume, M., Ueda, K., Nishiwaki, Y., Michikawa, T., Onozuka, D. (2010). Health effects of Asian dust events: A review of the literature. *Jpn. J. Hyg.* 65, 413–421. <https://doi.org/10.1265/jjh.65.413> (in Japanese with English Abstract)
- Hasunuma, H., Ichinose, T., Ueda, K., Odajima, H., Kanatani, K., Shimizu, A., Takami, A., Takeuchi, A., Nishiwaki, Y., Watanabe, M., Hashizume, M. (2019). Health effects of asian dust events: A literature review update of epidemiological evidence. *Jpn. J. Hyg.* 74, 19010. <https://doi.org/10.1265/jjh.19010> (in Japanese with English Abstract)
- Hersbach, H., Bell, B., Berrisford, P., Hirahara, S., Horányi, A., Muñoz-Sabater, J., Nicolas, J., Peubey, C., Radu, R., Schepers, D., Simmons, A., Soci, C., Abdalla, S., Abellan, X., Balsamo, G., Bechtold, P., Biavati, G., Bidlot, J., Bonavita, M., Chiara, G., *et al.* (2020). The ERA5 global reanalysis. *Q.J.R. Meteorol. Soc.* 146, 1999–2049. <https://doi.org/10.1002/qj.3803>
- Hongisto, M., Sofiev, M. (2004). Long-range transport of dust to the Baltic Sea region. *Int. J. Environ. Pollut.* 22, 72–86. <https://doi.org/10.1504/IJEP.2004.005493>
- Huang, J., Ji, M., Xie, Y., Wang, S., He, Y., Ran, J. (2016). Global semi-arid climate change over last 60 years. *Clim. Dyn.* 46, 1131–1150. <https://doi.org/10.1007/s00382-015-2636-8>
- Huang, J., Li, Y., Fu, C., Chen, F., Fu, Q., Dai, A., Shinoda, M., Ma, Z., Guo, W., Li, Z., Zhang, L., Liu, Y., Yu, H., He, Y., Xie, Y., Guan, X., Ji, M., Lin, L., Wang, S., Yan, H., *et al.* (2017). Dryland climate



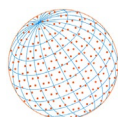
- change: Recent progress and challenges: Dryland Climate Change. *Rev. Geophys.* 55, 719–778. <https://doi.org/10.1002/2016RG000550>
- Hussein, T., Li, X., Al-Dulaimi, Q., Daour, S., Atashi, N., Viana, M., Alastuey, A., Sogacheva, L., Arar, S., Al-Hunaiti, A., Petäjä, T. (2020). Particulate matter concentrations in a Middle Eastern city – An insight to sand and dust storm episodes. *Aerosol Air Qual. Res.* 20, 2780–2792. <https://doi.org/10.4209/aaqr.2020.05.0195>
- Indoitu, R., Orlovsky, L., Orlovsky, N. (2012). Dust storms in Central Asia: Spatial and temporal variations. *J. Arid Environ.* 85, 62–70. <https://doi.org/10.1016/j.jaridenv.2012.03.018>
- Issanova, G., Abuduwaili, J., Kaldybayev, A., Semenov, O., Dedova, T. (2015). Dust storms in Kazakhstan: Frequency and division. *J. Geol. Soc. India* 85, 348–358. <https://doi.org/10.1007/s12594-015-0224-5>
- Issanova, G., Abuduwaili, J. (2017). *Aeolian Processes in the Arid Territories of Central Asia and Kazakhstan*. Springer Singapore, Singapore. <https://doi.org/10.1007/978-981-10-3190-8>
- Jickells, T.D., An, Z.S., Andersen, K.K., Baker, A.R., Bergametti, G., Brooks, N., Cao, J.J., Boyd, P.W., Duce, R.A., Hunter, K.A., Kawahata, H., Kubilay, N., laRoche, J., Liss, P.S., Mahowald, N., Prospero, J.M., Ridgwell, A.J., Tegen, I., Torres, R. (2005). Global iron connections between desert dust, ocean biogeochemistry, and climate. *Science* 308, 67–71. <https://doi.org/10.1126/science.1105959>
- Kang, J.H., Keller, J.J., Chen, C.S., Lin, H.C. (2012). Asian dust storm events are associated with an acute increase in pneumonia. *Ann. Epidemiol.* 22, 257–263. <https://doi.org/10.1016/j.annepidem.2012.02.008>
- Karaca, F., Anil, I., Alagha, O. (2009). Long-range potential source contributions of episodic aerosol events to PM₁₀ profile of a megacity. *Atmos. Environ.* 43, 5713–5722. <https://doi.org/10.1016/j.atmosenv.2009.08.005>
- Kashima, S., Yorifuji, T., Bae, S., Honda, Y., Lim, Y.H., Hong, Y.C. (2016). Asian dust effect on cause-specific mortality in five cities across South Korea and Japan. *Atmos. Environ.* 128, 20–27. <https://doi.org/10.1016/j.atmosenv.2015.12.063>
- Kaskaoutis, D.G., Houssos, E.E., Rashki, A., Francois, P., Legrand, M., Goto, D., Bartzokas, A., Kambezidis, H.D., Takemura, T. (2016). The Caspian Sea–Hindu Kush Index (CasHKI): A regulatory factor for dust activity over southwest Asia. *Glob. Planet. Change* 137, 10–23. <https://doi.org/10.1016/j.gloplacha.2015.12.011>
- Kaskaoutis, D.G., Rashki, A., Houssos, E.E., Legrand, M., Francois, P., Bartzokas, A., Kambezidis, H.D., Dumka, U.C., Goto, D., Takemura, T. (2017). Assessment of changes in atmospheric dynamics and dust activity over southwest Asia using the Caspian Sea–Hindu Kush Index. *Int. J. Climatol.* 37, 1013–1034. <https://doi.org/10.1002/joc.5053>
- Kaskaoutis, D.G., Francis, D., Rashki, A., Chaboureaud, J.P., Dumka, U.C. (2019). Atmospheric dynamics from synoptic to local scale during an intense frontal dust storm over the Sistan Basin in Winter 2019. *Geosciences* 9, 453. <https://doi.org/10.3390/geosciences9100453>
- Kismelyeva, S., Khalikhan, R., Torezhan, A., Kumisbek, A., Akimzhanova, Z., Karaca, F., Guney, M. (2021). Potential human exposure to mercury (Hg) in a chlor-alkali plant impacted zone: Risk characterization using updated site assessment data. *Sustainability* 13, 13816. <https://doi.org/10.3390/su132413816>
- Kok, J.F., Ridley, D.A., Zhou, Q., Miller, R.L., Zhao, C., Heald, C.L., Ward, D.S., Albani, S., Haustein, K. (2017). Smaller desert dust cooling effect estimated from analysis of dust size and abundance. *Nat. Geosci.* 10, 274–278. <https://doi.org/10.1038/ngeo2912>
- Kok, J.F., Ward, D.S., Mahowald, N.M., Evan, A.T. (2018). Global and regional importance of the direct dust-climate feedback. *Nat. Commun.* 9, 241. <https://doi.org/10.1038/s41467-017-02620-y>
- Lau, A.W.K., Shafiee, M., Smoot, G.F., Grossan, B., Li, S., Maksut, Z. (2020). On-sky silicon photomultiplier detector performance measurements for millisecond to sub-microsecond optical source variability studies. *JATIS* 6, 046002. <https://doi.org/10.1117/1.JATIS.6.4.046002>
- Laurent, B., Marticorena, B., Bergametti, G., Mei, F. (2006). Modeling mineral dust emissions from Chinese and Mongolian deserts. *Glob. Planet. Change* 52, 121–141. <https://doi.org/10.1016/j.gloplacha.2006.02.012>
- Li, Y., Song, Y., Kaskaoutis, D.G., Chen, X., Mamadjanov, Y., Tan, L. (2019). Atmospheric dust dynamics in southern Central Asia: Implications for buildup of Tajikistan loess sediments.



- Atmos. Res. 229, 74–85. <https://doi.org/10.1016/j.atmosres.2019.06.013>
- Li, Y., Song, Y., Kaskaoutis, D.G., Zan, J., Orozbaev, R., Tan, L., Chen, X. (2021). Aeolian dust dynamics in the Fergana Valley, Central Asia, since ~30 ka inferred from loess deposits. *Geosci. Front.* 12, 101180. <https://doi.org/10.1016/j.gsf.2021.101180>
- Liakakou, E., Stavroulas, I., Kaskaoutis, D.G., Grivas, G., Paraskevopoulou, D., Dumka, U.C., Tsagkaraki, M., Bougiatioti, A., Oikonomou, K., Sciare, J., Gerasopoulos, E., Mihalopoulos, N. (2020). Long-term variability, source apportionment and spectral properties of black carbon at an urban background site in Athens, Greece. *Atmo. Environ.* 222, 117137. <https://doi.org/10.1016/j.atmosenv.2019.117137>
- Madruza, D.G., Ubeda, R.M., Terroba, J.M., Dos Santos, S.G., García-Camero, J.P. (2019). Particle-associated polycyclic aromatic hydrocarbons in a representative urban location (indoor-outdoor) from South Europe: Assessment of potential sources and cancer risk to humans. *Indoor Air* 29, 817–827. <https://doi.org/10.1111/ina.12581>
- Maghrabi, A., Alharbi, B., Tapper, N. (2011). Impact of the March 2009 dust event in Saudi Arabia on aerosol optical properties, meteorological parameters, sky temperature and emissivity. *Atmos. Environ.* 45, 2164–2173. <https://doi.org/10.1016/j.ATMOSENV.2011.01.071>
- Mahmoodirad, A., Sanei, M. (2016). Solving a multi-stage multi-product solid supply chain network design problem by meta-heuristics. *Sci. Iran.* 23, 1428–1440.
- Mahmoodirad, A., Dehghan, R., Niroomand, S. (2019). Modelling linear fractional transportation problem in belief degree—based uncertain environment. *J. Exp. Theor. Artif. Intell.* 31, 393–408. <https://doi.org/10.1080/0952813X.2018.1552318>
- Mahowald, N., Albani, S., Kok, J.F., Engelstaeder, S., Scanza, R., Ward, D.S., Flanner, M.G. (2014). The size distribution of desert dust aerosols and its impact on the Earth system. *Aeolian Res.* 15, 53–71. <https://doi.org/10.1016/j.aeolia.2013.09.002>
- Martínez, M.A., Ruiz, J., Cuevas, E. (2009). Use of SEVIRI images and derived products in a WMO Sand and dust Storm Warning System. *IOP Conf. Ser. Earth Environ. Sci.* 7, 12004. <https://doi.org/10.1088/1755-1307/7/1/012004>
- Middleton, N.J. (2017). Desert dust hazards: A global review. *Aeolian Res.* 24, 53–63. <https://doi.org/10.1016/j.aeolia.2016.12.001>
- Middleton, N., Kang, U. (2017). Sand and Dust Storms: Impact Mitigation. *Sustainability* 9, 1053. <https://doi.org/10.3390/su9061053>
- Middleton, N. (2020). Health in dust belt cities and beyond—An essay by Nick Middleton. *BMJ* 371, m3089. <https://doi.org/10.1136/bmj.m3089>
- Middleton, N., Kashani, S.S., Attarchi, S., Rahnama, M., Mosalman, S.T. (2021). Synoptic causes and socio-economic consequences of a severe dust storm in the Middle East. *Atmosphere* 12, 1435. <https://doi.org/10.3390/atmos12111435>
- Miller, R., Cakmur, R., Perlwitz, J., Geogdzhayev, I., Ginoux, P., Koch, D., Kohfeld, K., Prigent, C., Ruedy, R., Schmidt, G., Tegen, I. (2006). Mineral dust aerosols in the NASA Goddard Institute for Space Sciences ModelE atmosphere general circulation model. *J. Geophys. Res.* 111, D06208. <https://doi.org/10.1029/2005JD005796>
- Ministry of Agriculture of the Republic of Kazakhstan (MARK) (2006). Analytical Report on Land Conditions and Use in the Republic of Kazakhstan. Committee of Land Administration of the Ministry of Agriculture of the Republic of Kazakhstan.
- Weather news from the world (MKWEATHER) (2021). Uzbekistan and southern Kazakhstan hit the worst dust storm in recorded history. <https://mkweather.com/uzbekistan-and-southern-kazakhstan-hit-the-worst-dust-storm-in-recorded-history/>
- Mohammadpour, K., Sciortino, M., Kaskaoutis, D., Rashki, A. (2022). Classification of synoptic weather clusters associated with dust accumulation over southeastern areas of the Caspian Sea (Northeast Iran and Karakum desert). *Aeolian Res.* 54, 100771. <https://doi.org/10.1016/j.aeolia.2022.100771>
- Molla-Alizadeh-Zavardehi, S., Mahmoodirad, A., Rahimian, M. (2014). Step fixed charge transportation problems via genetic algorithm. *Indian J. Sci. Technol.* 7, 949–954. <https://doi.org/10.17485/ijst/2014/v7i7.5>
- Niroomand, S., Harish Garg, H., Ali Mahmoodirad, A. (2020). An intuitionistic fuzzy two stage supply chain network design problem with multi-mode demand and multi-mode transportation. *ISA Trans.* 107, 117–133. <https://doi.org/10.1016/j.isatra.2020.07.033>



- Nobakht, M., Shahgedanova, M., White, K. (2021). New inventory of dust emission sources in central asia and northwestern China derived From MODIs imagery using dust enhancement technique. *J. Geophys. Res.* 126, e2020JD033382. <https://doi.org/10.1029/2020JD033382>
- National Program in the Republic of Kazakhstan (NPRK) (2005). National Program for the struggle against land desertification in the Republic of Kazakhstan for 2005–2015 years, Government Resolution # 49.
- Perez, L., Tobias, A., Querol, X., Künzli, N., Pey, J., Alastuey, A., Viana, M., Valero, N., González-Cabré, M., Sunyer, J. (2008). Coarse particles from saharan dust and daily mortality. *Epidemiology* 19, 800–807. <https://doi.org/10.1097/EDE.0b013e31818131cf>
- Prakash, P., Stenchikov, G., Kalenderski, S., Osipov, S., Bangalath, H.K. (2015). The impact of dust storms on the Arabian Peninsula and the Red Sea. *Atmos. Chem. Phys.* 15, 199–222. <https://doi.org/10.5194/acp-15-199-2015>
- Ramazanov, E., Lee, S.H., Lee, W. (2021). Stochastic risk assessment of urban soils contaminated by heavy metals in Kazakhstan. *Sci. Total Environ.* 750, 141535. <https://doi.org/10.1016/j.scitotenv.2020.141535>
- Rashki, A., Kaskaoutis, D.G., Francois, P., Kosmopoulos, P.G., Legrand, M. (2015). Dust-storm dynamics over Sistan region, Iran: Seasonality, transport characteristics and affected areas. *Aeolian Res.* 16, 35–48. <https://doi.org/10.1016/j.AEOLIA.2014.10.003>
- Rupakheti, D., Kang, S., Bilal, M., Gong, J., Xia, X., Cong, Z. (2019). Aerosol optical depth climatology over Central Asian countries based on Aqua-MODIS Collection 6.1 data: Aerosol variations and sources. *Atmos. Environ.* 207, 205–214. <https://doi.org/10.1016/j.atmosenv.2019.03.020>
- Rupakheti, D., Rupakheti, M., Abdullaev, S.F., Yin, X., Kang, S. (2020). Columnar aerosol properties and radiative effects over Dushanbe, Tajikistan in Central Asia. *Environ. Pollut.* 265, 114872. <https://doi.org/10.1016/j.envpol.2020.114872>
- Rupakheti, D., Rupakheti, M., Yin, X.F., Hofer, J., Rai, M., Hu, Y.L., Abdullaev, S.F., Kang, S.C. (2021). Modifications in aerosol physical, optical and radiative properties during heavy aerosol events over Dushanbe, Central Asia. *Geosci. Front.* 12, 101251. <https://doi.org/10.1016/j.gsf.2021.101251>
- Sayer, A.M., Hsu, N.C., Lee, J., Kim, W., Dutcher, S.T. (2019). Validation, stability, and consistency of MODIS Collection 6.1 and VIIRS Version 1 Deep Blue aerosol data over land. *J. Geophys. Res.* 124, 4658–4688. <https://doi.org/10.1029/2018JD029598>
- Schepanski, K., Tegen, I., Laurent, B., Heinold, B., Macke, A. (2007). A new Saharan dust source activation frequency map derived from MSG-SEVIRI IR-channels. *Geophys. Res. Lett.* 34, L18803. <https://doi.org/10.1029/2007GL030168>
- Schepanski, K., Tegen, I., Macke, A. (2009). Saharan dust transport and deposition towards the tropical northern Atlantic. *Atmos. Chem. Phys.* 9, 1173–1189. <https://doi.org/10.5194/acp-9-1173-2009>
- Schepanski, K. (2018). Transport of mineral dust and its impact on climate. *Geosciences* 8, 151. <https://doi.org/10.3390/geosciences8050151>
- Shafiee, M., Fegghi, S.A.H., Rahighi, J. (2017). Experimental performance evaluation of ILSF BPM data acquisition system. *Measurement* 100, 205–212. <https://doi.org/10.1016/j.measurement.2017.01.003>
- Shafiee, M., Grossan, B., Hu, J., Colantoni, I., Smoot, G. (2019). Design optimization of a 10 kilopixel optical band Microwave Kinetic Inductance Detector. *J. Instrument.* 14, P12011–P12011. <https://doi.org/10.1088/1748-0221/14/12/p12011>
- Shafiee, M., Fedorov, D., Grossan, B., Kizheppatt, V., Smoot, G. (2021). A readout system for microwave kinetic inductance detectors using software defined radios. *J. Instrument.* 16, P07015. <https://doi.org/10.1088/1748-0221/16/07/P07015>
- Shaheen, A., Wu, R., Aldabash, M. (2020). Long-term AOD trend assessment over the Eastern Mediterranean region: A comparative study including a new merged aerosol product. *Atmos. Environ.* 238, 117736. <https://doi.org/10.1016/j.atmosenv.2020.117736>
- Shi, L., Zhang, J.H., Yao, F., Zhang, D., Guo, H. (2019). Temporal variation of dust emissions in dust sources over Central Asia in recent decades and the climate linkages. *Atmos. Environ.* 222, 117176. <https://doi.org/10.1016/j.atmosenv.2019.117176>
- Solomos, S., Kalivitis, N., Mihalopoulos, N., Amiridis, V., Kouvarakis, G., Gkikas, A., Biniotoglou, I., Tsekeri, A., Kazadzis, S., Kottas, M., Pradhan, Y., Proestakis, E., Nastos, P.T., Marenco, F. (2018). From tropospheric folding to Khamsin and foehn winds: how atmospheric dynamics advanced



- a record-breaking dust episode in Crete. *Atmosphere* 9, 240. <https://doi.org/10.3390/atmos9070240>
- Song, Y., Li, Y., Cheng, L., Zong, X., Kang, S., Ghafarpour, A., Li, X., Sun, H., Fu, X., Dong, J., Mamadjanov, Y., Orozbaev, R., Shukurov, N., Gholami, H., Shukurov, S., Xie, M. (2021). Spatio-temporal distribution of quaternary loess across central Asia. *Palaeogeogr. Palaeoclimatol. Palaeoecol.* 567, 110279. <https://doi.org/10.1016/j.palaeo.2021.110279>
- Sternberg, T., Edwards, M. (2017). Desert dust and health: A central Asian review and steppe case study. *Int. J. Environ. Res. Public Health* 14, 1342. <https://doi.org/10.3390/ijerph14111342>
- Tegen, I., Lacis, A. (1996). Modeling of particle size distribution and its influence on the radiative properties of mineral dust aerosol. *J. Geophys. Res.* 101, 19237–19244. <https://doi.org/10.1029/95JD03610>
- Tositti, L., Brattich, E., Cassardo, C., Morozzi, P., Bracci, A., Marinoni, A., Di Sabatino, S., Porcù, F., Zappi, A. (2022). Development and evolution of an anomalous Asian dust event across Europe in March 2020. *Atmos. Chem. Phys.* 22, 4047–4073, <https://doi.org/10.5194/acp-22-4047-2022>
- United Nations (UN) (2010). United Nations News, Shrinking Aral Sea underscores need for urgent action on environment – Ban. <https://news.un.org/en/story/2010/04/334402>
- Uno, I., Eguchi, K., Yumimoto, K., Takemura, T., Shimizu, A., Uematsu, M., Liu, Z., Wang, Z., Hara, Y., Sugimoto, N. (2009). Asian dust transported one full circuit around the globe. *Nat. Geosci.* 2, 557–560. <https://doi.org/10.1038/NGEO583>
- Uzhydromet (2021). URL <https://hydromet.uz/>
- Wang, C.H., Chen, C.S., Lin, C.L. (2014). The threat of Asian dust storms on asthma patients: A population-based study in Taiwan. *Glob. Public Health* 9, 1040–1052. <https://doi.org/10.1080/17441692.2014.951871>
- Wang, F., Zhao, X., Gerlein-Safdi, C., Mu, Y., Wang, D., Lu, Q. (2017). Global sources, emissions, transport and deposition of dust and sand and their effects on the climate and environment: A review. *Front. Environ. Sci. Eng.* 11, 13. <https://doi.org/10.1007/s11783-017-0904-z>
- Wiggs, G., O'Hara, S., Wegerdt, J., Van Der Meer, J., Small, I., Hubbard, R. (2003). The dynamics and characteristics of aeolian dust in dryland Central Asia: Possible impacts on human exposure and respiratory health in the Aral Sea basin. *Geogr. J.* 169, 142–157. <https://doi.org/10.1111/1475-4959.04976>
- World Health Organization (WHO) (2006). WHO Air quality guidelines for particulate matter, ozone, nitrogen dioxide and sulfur dioxide : global update 2005 : summary of risk assessment. World Health Organization. <https://apps.who.int/iris/handle/10665/69477>
- Wu, Y., Wen, B., Li, S., Guo, Y. (2021). Sand and dust storms in Asia: A call for global cooperation on climate change. *Lancet Planetary Health* 5, e329–e330. [https://doi.org/10.1016/S2542-5196\(21\)00082-6](https://doi.org/10.1016/S2542-5196(21)00082-6)
- Xi, X., Sokolik, I.N. (2015). Dust interannual variability and trend in Central Asia from 2000 to 2014 and their climatic linkages. *J. Geophys. Res.* 120, 12175–12197. <https://doi.org/10.1002/2015JD024092>
- Zhang, X.X., Claiborn, C., Lei, J.Q., Vaughan, J., Wu, S.X., Li, S.Y., Liu, L.Y., Wang, Z.F., Wang, Y.D., Huang, S.Y., Zhou, J. (2020). Aeolian dust in Central Asia: Spatial distribution and temporal variability. *Atmos. Environ.* 238, 117734. <https://doi.org/10.1016/j.atmosenv.2020.117734>
- Zhou, C., Gui, H., Hu, J., Ke, H., Wang, Y., Zhang, X. (2019). Detection of new dust sources in central/East Asia and their impact on simulations of a severe sand and dust storm. *J. Geophys. Res.* 124, 232–247. <https://doi.org/10.1029/2019JD030753>